



January 2013

Performance Comparison Between Music And Esprit Algorithms For Direction Estimation Of Arrival Signals

Samira Kharel

Follow this and additional works at: <https://commons.und.edu/theses>

Recommended Citation

Kharel, Samira, "Performance Comparison Between Music And Esprit Algorithms For Direction Estimation Of Arrival Signals" (2013). *Theses and Dissertations*. 1557.
<https://commons.und.edu/theses/1557>

This Thesis is brought to you for free and open access by the Theses, Dissertations, and Senior Projects at UND Scholarly Commons. It has been accepted for inclusion in Theses and Dissertations by an authorized administrator of UND Scholarly Commons. For more information, please contact zeinebyousif@library.und.edu.

PERFORMANCE COMPARISON BETWEEN MUSIC AND ESPRIT ALGORITHMS FOR
DIRECTION ESTIMATION OF ARRIVAL SIGNALS

by

Samira Kharel
Bachelor of Engineering, Tribhuvan University, 2009

A Thesis
Submitted to the Graduate Faculty
of the
University of North Dakota
in partial fulfillment of the requirements

for the degree of
Master of Science


Grand Forks, North Dakota
December

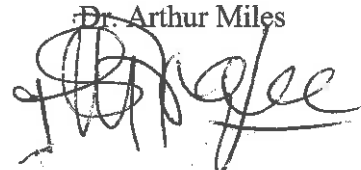
2013

Copyright 2013 Samira Kharel

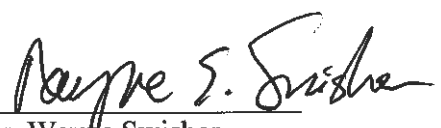
The Thesis, submitted by Samira Kharel in partial fulfillment of the requirements of the Degree of Master of Science from the University of North Dakota, has been read by the faculty advisory committee under whom the work has been done and is hereby approved.


Dr. Naima Kaabouch


Dr. Arthur Miles


Dr. Saleh Faruque

This thesis is being submitted by the appointed advisory committee as having met all of the requirements of the School of Graduate Studies at the University of North Dakota and is hereby approved.


Dr. Wayne Swisher
Dean of the School of Graduate Studies

November, 21, 2013
Date

PERMISSION

Title Performance Comparison between MUSIC and ESPRIT Algorithms for Direction Estimation of Arrival Signals

Department Electrical Engineering

Degree Master of Science

In presenting this thesis in partial fulfillment of the requirements for a graduate degree from the University of North Dakota, I agree that the library of this University shall make it freely available for inspection. I further agree that permission for extensive copying for scholarly purposes may be granted by the professor who supervised my thesis work or, in her absence, by the Chairperson of the department or the dean of the Graduate Studies. It is understood that any copying or publication or other use of this thesis or part thereof for financial gain shall not be allowed without my written permission. It is also understood that due recognition shall be given to me and to the University of North Dakota in any scholarly use which may be made of any material in my thesis.



Signature

11/15/2013

Date

TABLE OF CONTENTS

LIST OF FIGURES	viii
ACKNOWLEDGEMENTS	xiii
ABSTRACT	xiv
NOMENCLATURE	xv
CHAPTER	
I. INTRODUCTION	1
1.1 Evolution of Smart Antenna	2
1.1.1 Cell Splitting	4
1.1.2 Cell Sectoring	5
1.2 Smart Antenna Systems	6
1.2.1 Switched beam systems	7
1.2.2 Adaptive beam systems	9
1.3 Functional Block Diagram of Adaptive Array System	11
1.4 Adaptive Signal Processing Algorithms	12
1.5 DOA Algorithms	14
1.5.1 Spectral Estimation Methods	15
1.5.2 Eigen-structure DOA Methods / Subspace based methods	15

1.6 Beamforming	27
1.7 Hardware implementation for smart antenna.....	30
1.8 Summary.....	35
II. METHODOLOGY.....	37
2.1 MUSIC Algorithm	37
2.1.1 Flowchart for MUSIC.....	38
2.2 ESPRIT Algorithm.....	40
2.2.1 Flowchart for ESPRIT	40
2.3 Methodology for MATLAB	43
2.3.1 Function that were used while coding MUSIC and ESPRIT algorithms.....	43
2.4 Methodology for Simulink.....	45
2.4.1 Block diagram for MUSIC algorithm in Simulink	46
2.4.2 Block diagram for ESPRIT algorithm in Simulink.....	47
2.4.3 Blocks that were used for MUSIC and ESPRIT algorithms in Simulink	48
2.5 Summary.....	59
III. RESULTS AND ANALYSIS.....	60
3.1 Results from MATLAB	60
3.1.1 Error from MUSIC and ESPRIT with varying angle difference of signals.....	60
3.1.2 Error Vs. number of antenna elements	63
3.1.3 Error Vs. number of samples of signals.....	64

3.1.4 Ratio of MUSIC processing time to ESPRIT processing time with respect to number of arriving signals	66
3.1.5 Error vs. number of signals.....	67
3.1.6 Error with respect to SNR.....	68
3.2 Results from Simulink	69
3.2.1 Error vs angle difference.....	70
3.2.2 Error vs number of antenna elements	72
3.2.3 Error vs number of samples	73
3.2.4 Processing time and ratio of MUSIC processing time to ESPRIT processing time with Simulink.....	74
3.2.5 Error with different number of incoming signals	77
3.2.6 Error with SNR ratio.....	78
3.3 Analysis.....	79
IV. CONCLUSION AND RECOMMENDATIONS	81
4.1 Conclusion	81
4.2 Recommendations.....	82
REFERENCES	83

LIST OF FIGURES

Figure	Description	Page No.
1.1	Cellular structure with 7 cells reuse pattern	3
1.2	A schematic diagram of cell splitting	4
1.3	Sectorized base-station antenna	5
1.4	Co-channel interference comparison between (a) sectoring and (b) omnidirectional	6
1.5	Switched beam system	7
1.6	Comparison between (a) switched beam and (b) Adaptive array technique	8
1.7	Receive antenna selection	9
1.8	Coverage patterns for switched beam and adaptive array systems	10
1.9	Switched beam system using Butler matrix network for the beamforming	11
1.10	Functional block diagram of an adaptive array system	12
1.11	M X N planar array with graphical representation of time delay	13

1.12	M-element array with arriving signals	15
1.13	Four element linear element with two doublets	22
1.14	Reflectometer six ports	25
1.15	MUSIC spectrum for varying number of array elements	26
1.16	MUSIC spectrum for varying number of samples	27
1.17	N-element linear array	28
1.18	Two element array with desired and interfering signals	29
1.19	Block diagram of real-time DOA estimator VC33 prototype system	31
1.20	Equipment setup at transmitter site	31
1.21	Equipment setup at receiver site	32
1.22	Photograph of SDR platform	33
1.23	Block diagram of hardware configuration	33
1.24	Structure of the receiver	35
2.1	Flowchart of MUSIC algorithm	39
2.2	Flowchart of ESPRIT algorithm	42
2.3	Block diagram for MUSIC algorithm in Simulink	46

2.4	Block diagram for ESPRIT algorithm in Simulink	47
2.5	Random Source Block	48
2.6	Dialog box of Random Source	49
2.7	Gaussian Noise Generator Block	50
2.8	Dialog box of Gaussian Noise Generator	51
2.9	MATLAB Function Block	52
2.10	Editor for MATLAB Function block	53
2.11	Transpose Block	53
2.12	Dialog box of Transpose	54
2.13	Sign Block	54
2.14	Dialog box of Sign	55
2.15	Product Block	55
2.16	Dialog box of Product	56
2.17	Sqrt Block	57
2.18	Dialog box of Sqrt	57
2.19	Constant Block	58

2.20	Dialog box of Constant	58
3.1	Errors from MUSIC and ESPRIT algorithms vs angle difference between two input signals when number of antenna elements is 4	61
3.2	Errors from MUSIC and ESPRIT algorithms vs angle difference upto 10 between two input signals when number of antenna elements is 4	61
3.3	Errors vs angle difference between two input signals when number of antenna elements is 7	62
3.4	Error vs angle difference upto 10 between two input signals when number of antenna elements is 7	63
3.5	Errors from MUSIC and ESPRIT algorithm for different no. of antenna elements with two input signals	64
3.6	Error in angle estimation from MUSIC and ESPRIT algorithm for different no. of sample of signals	65
3.7	Error in angle estimation from MUSIC and ESPRIT algorithm for different no. of samples of signals upto 50	65
3.8	Ratio of MUSIC processing time to ESPRIT processing time vs number of signals	66
3.9	Processing time of MUSIC and ESPRIT in microseconds vs number of signals	67
3.10	Error from MUSIC and ESPRIT with respect to number of signals	68
3.11	Error from MUSIC and ESPRIT with respect to number of arriving signals	69
3.12	Error with respect to angle difference when number of antenna elements is 4 (with Simulink)	70
3.13	Error from MUSIC and ESPRIT with respect to angle difference when number of antenna elements is 7 (with Simulink)	71
3.14	Error from MUSIC and ESPRIT with respect to number of antenna elements (with Simulink)	72

3.15	Error from MUSIC and ESPRIT algorithms for different number of samples (with Simulink)	73
3.16	Error from MUSIC and ESPRIT algorithms for with respect to number of samples upto 50 (with Simulink)	74
3.17	Processing time of MUSIC and ESPRIT for angle estimation (with Simulink)	75
3.18	Ratio of processing time for MUSIC to ESPRIT with respect to number of incoming signals (with Simulink)	76
3.19	Error with respect to number of incoming signals (with Simulink)	78
3.20	Error with respect to SNR ratio (with Simulink)	79

ACKNOWLEDGEMENTS

I would first like to thank the University of North Dakota for providing me with an excellent opportunity to pursue my Master's program. I would like to thank my advisor Dr. Naima Kaabouch for her continual support as well as her guidance in the contents of the research which led to the timely completion of my thesis. Dr. Kaabouch has given me vast amount of ideas to conduct research efficiently for which I will be highly indebted to her throughout my life. I am very much indebted to the Professor Saleh Faruque and Professor Arthur Miles for their continual guidance and encouragement for the time during my master's program.

I would also like to thank my family members, my father Sudan Kharel, my mother Kamala Kharel, my brother Sameer Kharel and my sister Sabina Kharel whose continual emotional support has helped me to stay focused and organized. I am very much grateful to my friend Sanjib Tiwari for his continuous encouragement and help. Finally I would like to thank staffs of Department of Electrical Engineering, University of North Dakota for their continuous help.

ABSTRACT

This thesis examines and compares the performance of Multiple Signal Classification (MUSIC) and Estimation of Signal Parameters via Rotational Invariance Techniques (ESPRIT) for the estimation of Direction of Arrival (DOA) of incoming signals to the smart antenna. The comparison of these two algorithms was done on the basis of parameters like number of array elements, number of incoming signals, angle difference between the incoming signals, number of the samples taken of signal, processing time and SNR ratio.

These two algorithms were implemented with MATLAB and SIMULINK for the experimental purpose. After all the experiments performed, it was analyzed that results obtained from both of the software were almost same.

Comparing MUSIC's results with ESPRIT, it was found that MUSIC is less prone to error than ESPRIT for almost all parametric tests. This superiority of MUSIC made it desirable to recommend it for DOA estimation in smart antenna system.

NOMENCLATURE

a_{θ}	Array steering vector for the θ_i direction of arrival
A	Array steering vector
A_H	Hermitian transpose of A
A_1	Array steering vector for first subarray of antenna
A_2	Array steering vector for second subarray of antenna
d	Distance between two subarrays in the design for ESPRIT algorithm
dB	decibel
D	Number of signals
E_1	Signal subspace for first subarray
E_2	Signal subspace for second subarray
E_N	Noise eigenvector
I	Identity matrix
k	Free space wavenumber
K	Number of samples
M	Number of array elements
n	Noise vector
n^H	Hermitian transpose of n
n_1	Noise vector for first subarray of antenna
n_2	Noise vector for second subarray of antenna

P	Power spectrum
P_{MU}	MUSIC pseudospectrum
R_{nn}	Noise correlation matrix
R_{ss}	Source correlation matrix
R_{xx}	Array correlation matrix
s_i	Signal arriving to antenna system
s^H	Hermitian transpose of s
T	Unique nonsingular transformation matrix
w_m	Weight on the m^{th} array element
x	Input to antenna array
$x_i(k)$	Signal arriving in i^{th} element at k^{th} instant
x_1	Input to first subarray of antenna
x_2	Input to second subarray of antenna
y	Output of array
y_i	Output from i^{th} antenna element

Greek

Symbols

β	Phase shift between the elements
θ_i	Direction from which i^{th} signal arrived
λ_i	Diagonal elements of ϕ
ψ	Subspace rotation operator
ϕ	Diagonal unitary matrix with phase shifts between doublets for each

	DOA
σ^2	Noise variance

Abbreviations

ADC	Analog to Digital Converter
ADS	Advanced Design System
AF	Array Factor
BER	Bit Error Rate
CIR	Channel to Interference Ratio
DOA	Direction of Arrival
DSP	Digital Signal Processing
ESPRIT	Estimation of Signal Parameters via Rotational Invariance Technique
FPGA	Field Programmable Gate Array
IF	Intermediate Frequency
LNA	Low Noise Amplifier
LS	Least Square
MATLAB	MATrix LABoratory
MSE	Mean Square Error
MUSIC	MUltiple SIgnal Classification
RF	Radio Frequency
RORM	Reduced Order Root MUSIC
SDMA	Space Division Multiple Access
SDR	Software Defined Radio

SINR	Signal to Interference plus Noise Ratio
SNR	Signal to Noise Ratio
SSM	Spatial Smoothing MUSIC

CHAPTER I

INTRODUCTION

The increasing demand for higher wireless communication bandwidth and better transmission / reception capabilities has urged researchers to develop techniques that improve the performance of wireless radio systems. Smart antennas have recently received a lot of interest as a good solution that can enhance the received signal, suppress all interfering signals, and increase capacity. Other techniques have also been proposed to increase channel capacity and deal with signal interference include cell splitting and cell sectoring. However, these methods are not efficient in dynamic networks such as, moving ground vehicles or aircraft.

The idea of smart antenna is based on spatial diversity where multiple antennas are strategically spaced and connected to a common transceiver system. This type of antenna has the capability to adapt the shape of the beam in the desired direction. The pattern of smart antenna is controlled using a signal processing algorithm in the basis of different criteria such as: maximizing the signal to interference ratio, steering the beam in the direction of desired signal, nullifying the inference signals, and adapting the beam with the moving emitter.

In this thesis two subspace based algorithms that are Multiple Signal Classification (MUSIC) and Estimation of Signal Parameters via Rotational Invariance Techniques (ESPRIT) are studied in detail and then compared for the estimation of Direction of Arrival (DOA) of incoming signals to

the smart antenna. The concept of subspace based methods is to exploit the eigenvalues and eigenvectors of the auto correlation matrix of array to find DOA of signals.

1.1 Evolution of Smart Antenna

Though the technology of smart antenna seems to be the new technology but they were already been implemented in defense-related system since World War II [1].

To overcome the day by day increasing demand in the field of wireless communication lead researchers to move toward the development of smart antenna technology. To meet this demand high advanced system which involves signal processing method was developed and known as smart antenna as they act smart due to the signal processing. Smart antenna improves channel capacity and spectrum efficiency, extends range coverage, and also reduces delay spread, multipath fading, co-channel interference, system error, bit error rate (BER) and outage probability [2].

The evolution of this technology started seeding with the introduction of cellular concept in the field of wireless communication. The cellular concept is a system-level idea which calls for replacing a single, high power transmitter (large cell) with many low power transmitters (small cells), each providing coverage to only a small portion of the service area [3].

Each shaded hexagonal area in fig. 1.1 represents a small geographical area named *cell* with maximum radius R . Each cell has a base station at its center equipped with an omnidirectional antenna with a given band of frequencies.

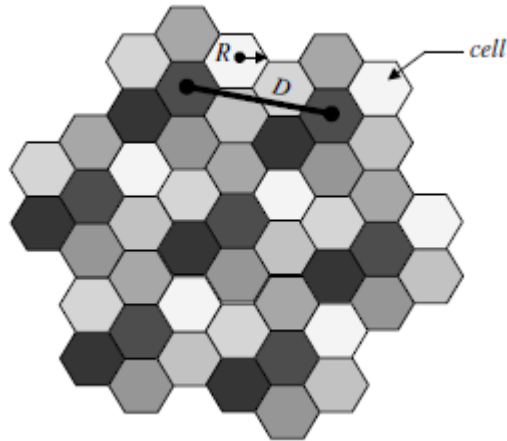


Figure 1.1: Cellular structure with 7 cells reuse pattern

Base stations in adjacent cells are assigned frequency bands that contain different frequencies compared to the neighboring cells. By limiting the coverage area to within the boundaries of a cell, the same band of frequencies may be used to cover different cells that are separated from one another by distances large enough to keep interference levels below the threshold of the others. The concept of reusing the same bands of frequencies to different cells of cellular base stations within a system is referred to as frequency reuse, and cells that use the same set of frequencies are known as co-channel cells. A set of N cells which collectively use the same set of available frequencies is called a cluster. This concept is shown in fig. 1.1 by repeating shaded clusters, and also the shaded region separated by distance D in fig. 1.1 are co-channel cells.

At the beginning of implementation of cellular concept, omnidirectional antennas were equipped in each base station. As an omnidirectional antenna has tendency to radiate radio wave power uniformly in all directions, only a small percentage of the total energy reached the desired user, rest of the energy were radiated in undesired directions. So these co-channel cells separated with distance D are the one which are most affected by the interference from the co-channel, also

known as the co-channel interference. And as the number of the interference increases it decreases the capacity of the channel.

Hence, different methods like cell splitting and cell sectorization were developed to overcome the capacity demand in cellular communication [1].

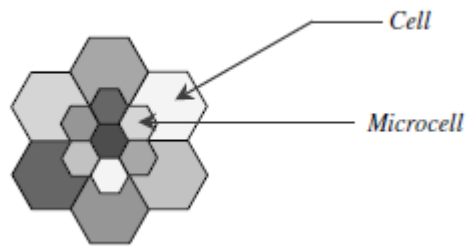


Figure 1.2: A schematic diagram of cell splitting

1.1.1 Cell Splitting

Cell splitting, as shown in fig. 1.2, subdivides a congested cell into smaller cells, called microcells, each having its own base station and hence corresponding reduction in antenna height and transmitter power. Cell splitting improves capacity by decreasing the cell radius, R , and keeping the D/R ratio unchanged. The disadvantages of cell splitting are the costs incurred from the installation of new base stations, the increase in the number of handoff (the process of transferring communication to a new base station when the mobile unit travels from one cell to another), and a higher processing load per subscriber.

As the demand for wireless service grew even higher, the number of frequencies assigned to a cell eventually became insufficient to support the required number of subscribers. Thus, a cellular design technique was needed to provide more frequencies per coverage area. This technique is called cell sectoring [3], where a single omnidirectional antenna at the base station is replaced with several directional antennas.

1.1.2 Cell Sectoring



Figure 1.3: Sectorized base-station antenna

Fig. 1.3 shows the cell sectoring technique considering a cell sectorized into three sectors of 120° each [1]. In sectoring, capacity is improved while keeping the cell radius unchanged and reducing the D/R ratio. In other words, by reducing the number of cells in a cluster and thus increasing the frequency reuse, capacity improvement is achieved.

Sectorization reduces the co-channel interference in cellular systems since it uses directional antenna that radiates in only one particular direction with certain beam angle. The factor by which the interference is reduced depends on the amount of sectoring used [1]. Fig. 1.4 compares the interference between omnidirectional and sectoring where the cells have been sectorized into three 120° sectors. Here, only two neighboring cells interfere, instead of six for the omnidirectional case. Though these methods increase the signal to interference (S/I) ratio and also increases the capacity of channel, the side effects of this method is the increase in number of antennas at each base station, and decrease in trunking efficiency due to channel sectoring at each base station.

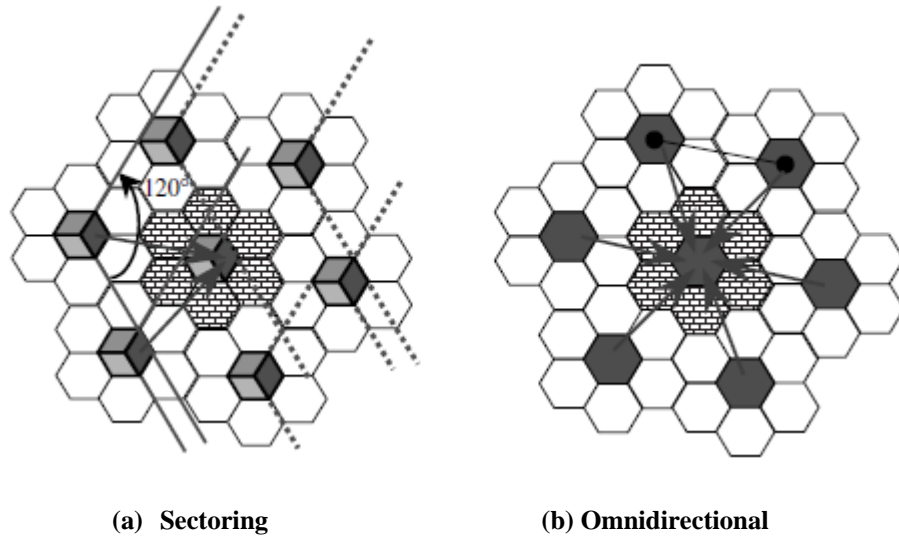


Figure 1.4: Co-channel interference comparison between (a) sectoring and (b) omnidirectional

1.2 Smart Antenna Systems

Despite its benefits, cell sectoring did not provide the solution needed for the capacity problem. Therefore, the system designers began to look into a system that could dynamically sectorize a cell. Hence, they began to examine smart antennas.

Smart antenna systems are basically an extension of cell sectoring in which the sector coverage is composed of multiple beams [4]. This is achieved by the use of antenna arrays, and the number of beams in the sector is a function of the array geometry. Because smart antennas can focus their radiation pattern toward the desired users while rejecting unwanted interferences, they can provide greater coverage area for each base station. Moreover, because smart antennas have a higher interference rejection, and therefore lower bit error rate (BER), they can provide a substantial capacity improvement. These systems can generally be classified as either Switched-Beam or Adaptive Array [1], [2], [4].

1.2.1 Switched beam systems

This is the further enhancement of the cell sectorization. It consists of highly directive and predefined fixed beams formed with an array of antenna. Fig. 1.5 shows the figure of switched beam system. This system continuously scans the signal strength as the user moves throughout the cell. The beam that gives the highest signal strength is selected and the system continually switches the beam if necessary. As the beam that gives the highest signal strength is selected for the communication, signal to interference plus noise ratio (SINR) is significantly improved. Depending on the environmental circumstance and hardware/software used, this system can increase base station range from 20 to 200% over the conventional cell sectorization system [2].

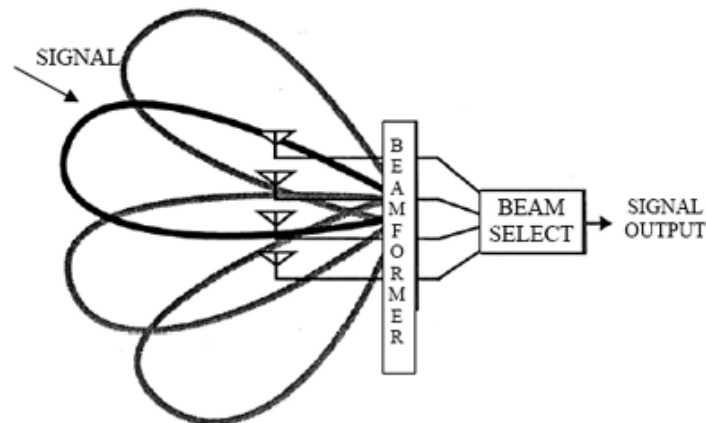


Figure 1.5: Switched beam system

Ho et al. (1998) presented the idea of implementing the switched beam smart antenna for cellular radio system to enhance the performance of the whole system [5]. From their experiments they concluded that, with the usage of multiple directional antennas with switched beam methodology in the system, channel to interference ratio (CIR) decreased while increasing trunking efficiency.

Though this system enhances overall system performance, since the beams are fixed, the intended user may not be in the center of any given main beam [4]. If there is an interferer near

the center of the active beam, it may be enhanced more than the desired user [6]. Hence, this system works well only in the environment where there is less number of interferers.

The comparison between the beamforming lobes of switched beam system and the adaptive array system is shown in the fig. 6[4].

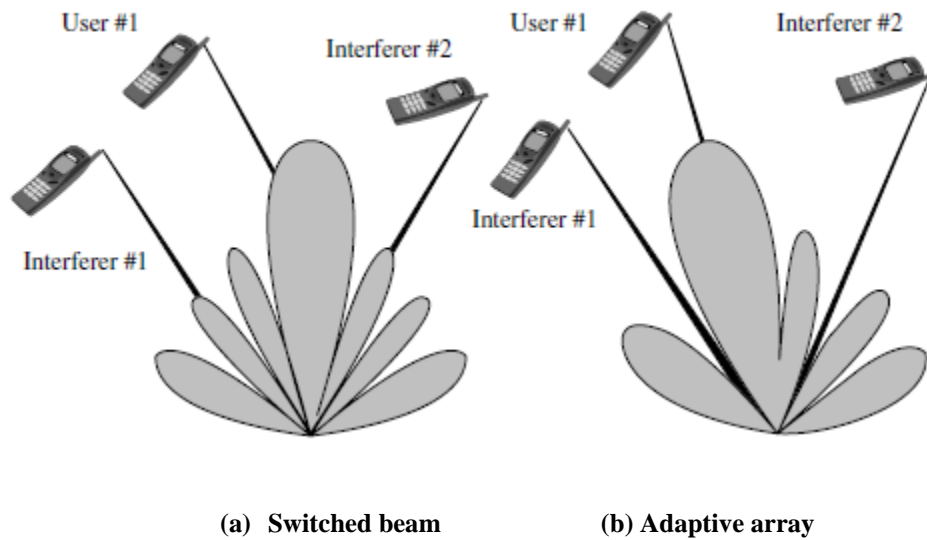


Figure 1.6: Comparison between (a) switched beam and (b) Adaptive array technique [4]

Sanayei et al. (2004) presented the idea of antenna selection from a set of multiple antennas [7]. They shared the idea of selecting the antenna with highest signal to noise ratio (SNR) which is based in the concept of switched beam system.

They considered two cases for the receptions; in the first one there is only one RF chain in the receiver side. In this case, the receiver scanned the antennas and found the antenna with the highest SNR and selected it for the reception of next data burst. Fig. 1.7 shows receive antenna selection for the system.

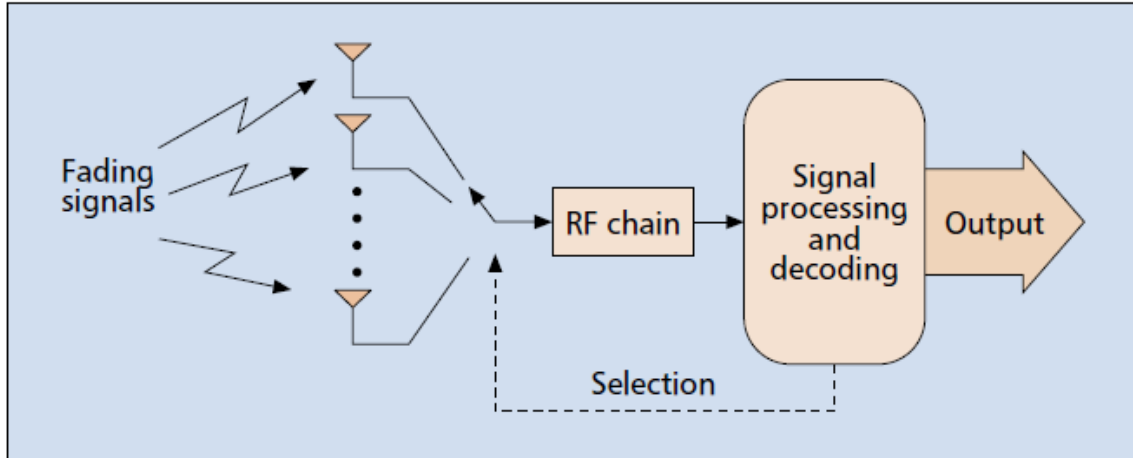


Figure 1.7: Receive antenna selection [7]

The other case was selecting set of fixed number of antennas in corresponding to the number of available RF channels. This selection was based on the SNR of the antenna, i.e. antenna with the highest SNR was selected.

The idea presented by them reduces hardware complexity; achieve full diversity along with the cost reduction. With these advantages there are still several drawbacks in their system like the selection might not be feasible whenever the channel are highly frequency selective and also due to the attenuation caused by practical switches implemented in the system.

1.2.2 Adaptive beam systems

Adaptive beam system provides more degrees of freedom since they have the ability to adapt the radiation pattern to the RF signal environment in real time. These systems are more digital processing intensive than switched beam system [1], [4].

In adaptive beam system, DOA of incoming signals is computed first then the array's beam pattern is formed in such a way that the maximum of the beam pattern is in the direction of desired user and nulls toward the interferers [2]. In other words, adaptive array systems can

customize an appropriate radiation pattern for each individual user [4]. This is far superior to the performance of a switched-beam system, it can also be seen from fig. 1.6. This figure shows that not only the switched-beam system may not be able to place the desired signal at the maximum of the main lobe but also it exhibits the inability to fully reject the interferers.

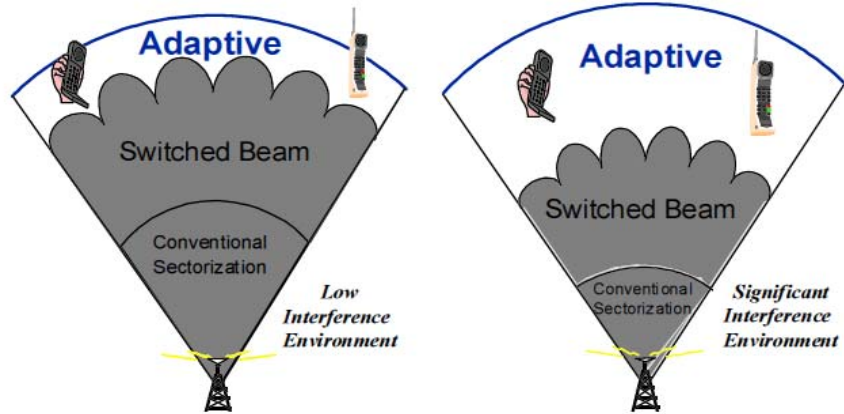


Figure 1.8: Coverage patterns for switched beam and adaptive array systems [8]

Because of the ability to control the overall radiation pattern in a greater coverage area for each cell site, as illustrated in fig. 1.8, adaptive array systems greatly increase capacity. Fig. 1.8 shows a comparison, in terms of relative coverage area, of conventional sectorized switched-beam and adaptive arrays system.

Fakoukakis et al. (2005) presented the idea of switched beam smart antenna system using Butler matrix method for the better performance [13]. Fig. 1.9 shows the switched beam system they implemented using Butler matrix method for the beamforming. They also presented the idea to combine the concept of switched beam and adaptive beam smart antenna. From their study, though they found out that the adaptive beam smart antenna methodology improved the performance of the whole system, they suggested switched beam method for next generation SDMA schemes as adaptive beam method is harder to implement and is costly.

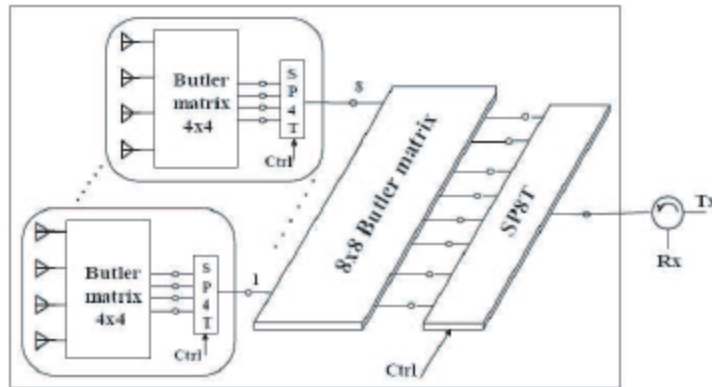


Figure 1.9: Switched beam system using Butler matrix network for the beamforming [13]

So, from these analyses it can also be said that, in the environment of low inference switched beam system can be used as it is less complex as well as cheaper than adaptive arrays system, while for the environment of high interference adaptive arrays system should be implemented.

1.3 Functional Block Diagram of Adaptive Array System

Fig. 1.10[4] shows the functional block diagram of an adaptive array system. This block diagram shows that the RF signals from N antennas are down converted to a baseband/IF frequency and then digitized. This system then locates the DOA of the desired signal as well as of signals that are not of interest using the DOA algorithms. After the estimation of the DOA of signals, processor adapts it beam towards the direction of the desired signal and nullifies the beam in the direction of the interfering signal, and also it continuously tracks the signal of interest and signals that are not of interest by dynamically changing the complex weight of the system.

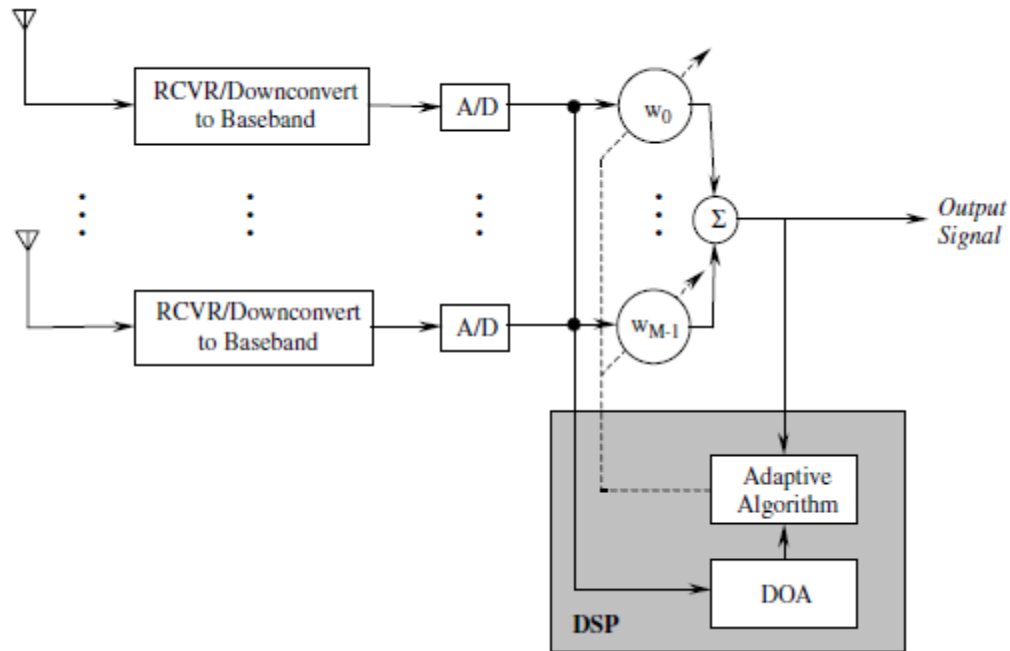


Figure 1.10: Functional block diagram of an adaptive array system [4]

1.4 Adaptive Signal Processing Algorithms

The development of adaptive arrays began in the late 50s and has been more than four decades in the making. The word *adaptive array* was first coined by Van Atta, in 1959, to describe a self-phased array [16]. To get the adaptive array system, as mentioned before, first of all the DOA of desired signal as well as interfering signals should be known and then with the knowledge of DOA of incoming signals, radiation pattern of the array is adapted in such a way that its maximum points towards the desired user and nulls towards the interfering signals. The process of formation of radiation pattern or beam in this way is known as beamforming. There are different algorithms developed to find DOA of the incoming signals and for beamforming.

Bellofiore et al (August 2002) have discussed about the time delay method which is the basis for DOA algorithm to determine the directions of all incoming signals in detail [17]. They have

explained that the classical methods are based on the concept of measuring power received from each direction. These algorithms determine the angles of arrival of the incoming signals by scanning the beam of the radiation pattern, and surveying the space for the signals above a certain power threshold. These methods are known as low-resolution algorithms.

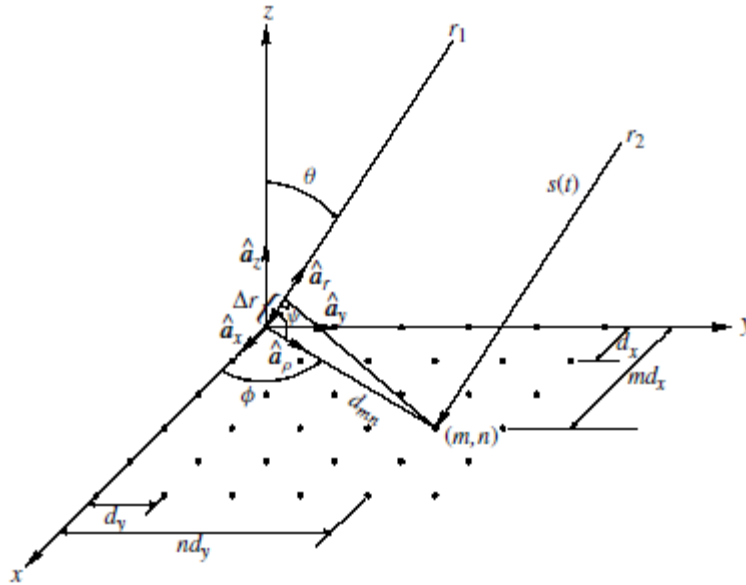


Figure 1.11: M X N planar array with graphical representation of time delay [17]

Fig. 1.11 shows M x N planar array, with inter-element spacing d_x along x axis, and d_y along the y axis [17]. When an incoming wave, carrying a baseband signal $s(t)$, impinges at an angle (θ, ϕ) on the antenna array, it produces time delays relative to the signal received at the other antenna elements. These time delays depend on the antenna geometry, the number of elements, and the spacing between the elements. For the array of fig. 1.11, they considered the time delay of the signal $s(t)$ at the (m,n) th element relative to the reference element $(0,0)$, at the origin is

$$\tau_{mn} = \frac{\Delta r}{v_0} \quad \text{equation (1.1)}$$

where Δr and v_0 are the differential distance and the speed of the light in free space respectively.

After the computation of equation (1.1) the time delay is obtained as

$$\tau_{mn} = \frac{md_x \sin\theta \cos\phi + nd_y \sin\theta \sin\phi}{v_0} \quad \text{equation (1.2)}$$

where m and n are the (m,n) th element of the array respectively.

1.5 DOA Algorithms

There are many DOA estimation techniques developed till this date. There are several methods for estimating the Direction of Arrival. DOA estimation techniques can be categorized on the basis of the data analysis and implementation into four different areas: conventional methods, subspace-based methods, maximum likelihood methods, and integrated methods, which combine property restoral techniques with subspace-based approach.

Conventional methods for DOA estimation are based on the concepts of beamforming and null steering and do not exploit the statistics of the received signal. In this technique, the DOA of all the signals is determined from the peaks of the output power spectrum obtained from steering the beam in all possible directions. Examples of conventional methods are the delay-and-sum method (classical beamformer method or Fourier method) and Capon's minimum variance method. One major disadvantage of the delay-and-sum method is its poor resolution; that is, the width of the main beam and the height of the side lobes limit its ability to separate closely spaced signals [20]. On the other hand, Capon's minimum variance technique tries to overcome the poor resolution problem associated with the delay-and-sum method, and in fact, it gives a significant improvement. Although it provides better resolution, Capon's method fails when the interfering signals are correlated with the desired signal.

On the basis of the way they are computed DOA estimation methods can also be sorted into two categories: Spectral Estimation Methods and Eigenstructure DOA Methods.

1.5.1 Spectral Estimation Methods

Spectral Estimation Methods first compute a spatial spectrum, and then estimate DOAs by localizing maxima of this spectrum. These methods apply weights to each element in the array in order to point the antenna pattern towards a known look direction. The received power is then estimated for a large number of look directions and the look directions with maximum received power are chosen as the DOAs. Variants of the spectral estimation methods differ by how the weights are calculated to steer the main beam. Methods that fall under this class of DOA estimators include the Maximum Likelihood method, Bartlett Method and the Linear Prediction Method. These methods are simple, but suffer from lack of resolution. For this reason, the high resolution Eigen-structure methods are more often used than Spectral Estimation Methods.

1.5.2 Eigen-structure DOA Methods / Subspace based methods

The eigen-structure DOA methods depend on the eigenvalues and eigenvectors of the array correlation matrix [16]. Fig. 1.12 depicts a typical scenario where D signals (s_1, s_2, \dots, s_D) arriving from D different directions ($\theta_1, \theta_2, \dots, \theta_D$) impinge a M element array with M different weights (w_1, w_2, \dots, w_M). In these methods it is assumed that $D < M$. Each array element receives the $x_m(k)$ signal in the k^{th} instant, which includes additive, zero mean, Gaussian noise.

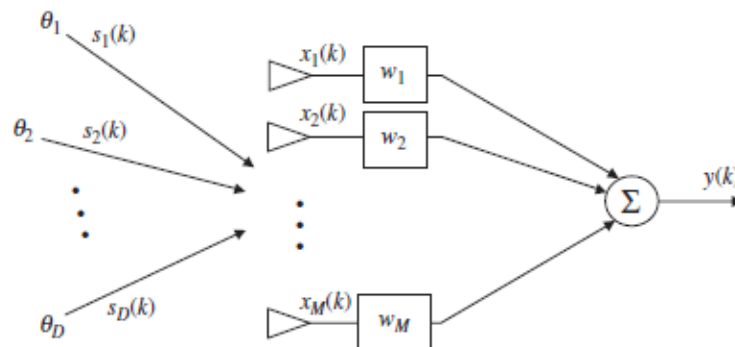


Figure 1.12: M-element array with arriving signals [16]

Output y for this array will be,

$$y(k) = w^T \cdot x(k) \quad \text{equation (1.3)}$$

where,

$$x(k) = [a(\theta_1) \ a(\theta_2) \ \dots \ a(\theta_D)] \cdot \begin{bmatrix} s_1(k) \\ s_2(k) \\ \vdots \\ s_D(k) \end{bmatrix} + n(k)$$

$$= As(k) + n(k) \quad \text{equation (1.4)}$$

and

$$w(k) = [w_1 \ w_2 \ \dots \ w_M]^T = \text{array weights}$$

$s(k)$ = vector of incident complex monochromatic signals at time k

$n(k)$ = noise vector at each array element m , zero mean, variance σ_n^2

$a(\theta_i)$ = M -element array steering vector for the θ_i direction of arrival

$A = [a(\theta_1) \ a(\theta_2) \ \dots \ a(\theta_D)]$ $M \times D$ matrix of steering vectors $a\theta_i$

The array correlation matrix will be,

$$\begin{aligned} R_{xx} &= E[x \cdot x^H] = E[(As + n)(s^H A^H + n^H)] \\ &= AE[s \cdot s^H]A^H + E[n \cdot n^H] \\ &= AR_{ss}A^H + R_{nn} \end{aligned} \quad \text{equation (1.5)}$$

where,

$R_{ss} = D \times D$ source correlation matrix

$R_{nn} = \sigma_n^2 I = M \times M$ noise correlation matrix

$I = N \times N$ identity matrix

Here, H in superscript denotes Hermitian Transpose I for identity matrix. The time averaged correlation matrix for signal and noise is computed as follows,

$$R_{ss} \approx \frac{1}{K} \sum_{k=1}^K s(k)s^H(k) \quad R_{nn} \approx \frac{1}{K} \sum_{k=1}^K n(k)n^H(k)$$

When the signals are uncorrelated, R_{ss} will be a diagonal matrix as off-diagonal elements have no correlation. R_{ss} will be a non-singular matrix when the signals are partly correlated. When the signals are coherent, R_{ss} becomes singular.

The eigenstructure DOA methods use two properties of the correlation matrix R_{xx} for estimating the angle of arrival. First, the space spanned by its eigenvectors can be partitioned into two subspaces, namely, the signal subspace and the noise subspace. Second, vectors that correspond to directional sources are orthogonal to the noise subspace, and are contained in the signal subspace. Therefore, it is possible to find vectors corresponding to the direction of sources. Basically, Eigen-structure techniques look for directions whose steering vectors are orthogonal to the noise subspace and are contained in the signal subspace. Two of the most popular Eigen-structure methods are the ESPRIT (Estimation of Signal Parameters via Rotational Invariance Techniques) and MUSIC (Multiple Signal Classification) algorithms, these methods have shown excellent accuracy and resolution in many experimental and theoretical studies.

This chapter gives a detailed overview of MUSIC and ESPRIT for the estimation of DOA. As these algorithms exploit the eigenvector of noise and signal they are also called subspace based methods.

1.5.2.1 MUSIC Algorithm

Schmidt (1986) proposed the idea of MUSIC algorithm which is a high resolution subspace based method. MUSIC is an acronym which stands for MULTIPLE SIGNAL CLASSIFICATION. When the array is well calibrated and the signals are uncorrelated, MUSIC provides unbiased estimates of the number of signals, the angles of arrival, and the strengths of the waveforms. Because MUSIC assumes that the noise in each channel is uncorrelated, the noise correlation matrix is diagonal. Since the incident signals are either somewhat correlated or uncorrelated, the signal correlation matrix is not necessarily diagonal. This method implies either to know in advance the number of incoming signals or to search the eigenvalues to determine the number of incoming signals.

If the number of signals is D , the number of signal eigenvalues and eigenvectors is D , and the number of noise eigenvalues and eigenvectors is $M - D$ (M is the number of array elements). By assuming uncorrelated noise with equal variances, the array correlation matrix becomes:

$$R_{xx} = A * R_{ss} * A^H + \sigma_n^2 I \quad \text{equation (1.6)}$$

R_{xx} is an $M \times M$ matrix. After computation of array correlation matrix, R_{xx} , we have to find the eigenvalues and eigenvectors for R_{xx} . From the eigenvectors computed, D eigenvectors are associated with the signals and $M - D$ eigenvectors are associated with the noise. We further deal with the $M - D$ eigenvectors associated with the noise that have smallest corresponding $M - D$ eigenvalues from the set of eigenvalues of R_{xx} . For uncorrelated signals, the smallest eigenvalues

are equal to the variance of the noise. Hence, equation (1.7) defines the $M \times (M-D)$ dimensional subspace composed by the noise eigenvectors associated with the smallest eigenvalues.

$$E_N = [e_1 \ e_2 \ \dots \ e_{M-D}] \quad \text{equation (1.7)}$$

The eigen-vectors of the noise subspace ($\bar{e}_1, \bar{e}_2, \dots, \bar{e}_{M-D}$) are orthogonal to the array steering vectors at the angles of arrival $\theta_1, \theta_2, \dots, \theta_D$. Due to this orthogonality, the Euclidean distance $d^2 = \mathbf{a}(\theta)^H E_N E_N^H \mathbf{a}(\theta) = 0$ for each and every arrival angle $\theta_1, \theta_2, \dots, \theta_D$. Substituting this distance expression in the denominator of equation (1.8) of MUSIC pseudospectrum given below creates sharp peaks at the angles of arrival.

$$P_{MU}(\theta) = 1/ |\mathbf{a}(\theta)^H E_N E_N^H \mathbf{a}(\theta)| \quad \text{equation (1.8)}$$

Weber et al (2009) have derived the equation for Capon as well as MUSIC and then compared them with each other [21]. Capon output power spectrum from their derivation is

$$P_{MU}(\theta) = 1/ |\mathbf{a}^H(\theta) \mathbf{R}_{xx}^{-1} \mathbf{a}(\theta)| \quad \text{equation (1.9)}$$

where, $\mathbf{a}(\theta)$ is steering vector for angle θ and \mathbf{R} is array correlation matrix.

After the derivation of output power spectrum they compared both algorithms and found out that MUSIC gives more accurate result than Capon when angle difference between two signals is very less. Also, angle estimation from MUSIC is more accurate than Capon for the array with small number of antenna elements while both algorithms perform well when number of antenna elements in array is large.

Vesa (2010) has done analysis along with the derivation of equation for MUSIC algorithm and Root-MUSIC algorithm [24]. Root-MUSIC is also based on eigen-analysis of the array correlation matrix as MUSIC algorithm. This algorithm implies that the MUSIC algorithm is

reduced to finding roots of a polynomial as opposed to merely plotting the pseudospectrum or searching for peaks in the pseudospectrum [16]. Vesa (2010) did extensive computer simulation to demonstrate the performances of the MUSIC and Root-MUSIC algorithm. He observed that the Root-MUSIC algorithm is not so powerful, but in some cases the results obtained with this algorithm are acceptable. According to him these two algorithms enhances the DOA estimation. With use of MUSIC algorithms smart antennas add a new possibility of user separation by space through Space Division Multiple Access (SDMA).

Rao et al. (2011) has implemented MUSIC algorithm for the estimation of angle of arrival and they also studied the response of the algorithm with change in different parameters [25]. They did the parametric test for static and dynamic cases. For static case they changed the value of SNR and observed the response from the plot of MATLAB. It was concluded from their observation that the information of angle of arrival is more accurate with the high SNR. The bandwidth of the angle does increases with the decrease in SNR.

Rao et al. (2011) observation from dynamic case study showed that, in the case of moving user i.e. dynamic angle of arrivals, with increase in samples of input signals with respect to time the accuracy of result also increases.

R.S. Kawitkar et al. (2005) presented the idea of MUSIC algorithm for the estimation of arrival angles [28]. They compared the resolution of power spectral density with respect to angle for different angle estimation methods like spectral estimator, maximum likelihood, linear predictor and MUSIC algorithm. While the observation of their result, it was found that spectral estimator method has the poorest resolution. Compared to spectral estimator method, maximum likelihood and linear predictor methods have the better resolution, and also all above these methods MUSIC algorithm gave the best estimation of arrival angles with best resolution from their experiment.

Rao et al. (2012) did experiment on the performance of smart antenna with real data of the received signals from the experimental setup that includes hardware part [30]. Linear uniform array of antenna was used as a sensor for the input signals. With these real data from the real environment, angle of arrivals were estimated using MUSIC algorithm.

The output response they obtained was for spectrum (P), log (P) and its derivative with respect to the angle. At the angle of arrivals these parameters do have maximum peak and for the derivative plot there is zero crossing in these arrival angles.

They also presented that if there are multiple users which have same angle of arrival, then the smart antenna system can detect only one of the user as one will mask over the other. Their experiment also showed that, in the case of dynamic angle of arrival, it is always better to take more samples for more précised response.

1.5.2.2 ESPRIT Algorithm

Roy et al. (1989) proposed the idea of ESPRIT algorithm that has significant performance and computational advantages over previous algorithms for estimation of arrival angles. ESPRIT stands for Estimation of Signal Parameters via Rotational Invariance Techniques which is another subspace based DOA estimation algorithm. It does not involve an exhaustive search through all possible steering vectors to estimate DOA and hence reduces the computational and storage requirements in large extent compared to MUSIC. ESPRIT exploits an underlying rotational invariance among signal subspaces induced by an array of sensors with a translational invariance structure.

Roy et al. (1989) designed the array of antenna which was divided into subarrays of antenna also known as doublets which have identical sensitivity patterns and were translationally separated by

a known constant vector [32]. Doublets can be separate arrays or can be composed of subarrays of one larger array. After the calculation of the correlation matrix for these subarrays, signal subspaces for both were computed. Since these subarrays are translationally related, the subspaces of eigenvectors are related by a unique non-singular transformation matrix. With the information of this transformation matrix or rotational operator that maps signal subspace of one subarray into signal subspace of other, the estimation of arrival angles was done.

Fig. 1.13 shows an example of four element linear array composed of two identical three element subarrays or two doublets.

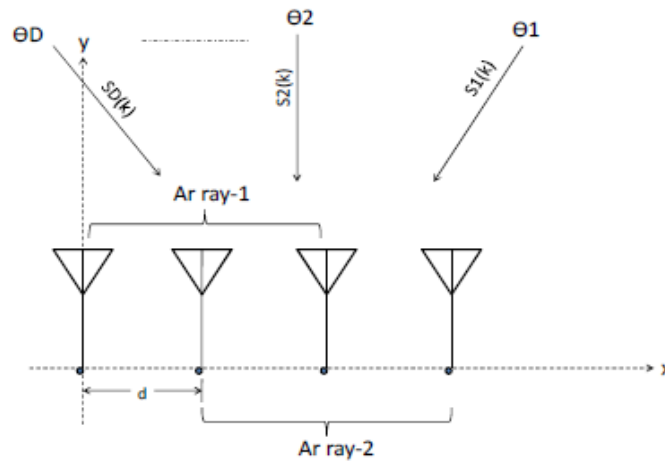


Figure 1.13: Four element linear element with two doublets

These two subarrays, array 1 and array 2 are translationally displaced by the distance ‘d’. The signal induced in each of the array is given by,

$$x_1(k) = [a(\theta_1) \ a(\theta_2) \ \dots \ a(\theta_D)] \cdot \begin{bmatrix} s_1(k) \\ s_2(k) \\ \vdots \\ s_D(k) \end{bmatrix} + n_1(k)$$

$$= A_1 \cdot s(k) + n_1(k) \quad \text{equation (1.10)}$$

and

$$\begin{aligned} x_2(k) &= A_2 \cdot s(k) + n_2(k) \\ &= A_1 \cdot \phi \cdot s(k) + n_2(k) \end{aligned} \quad \text{equation (1.11)}$$

where,

$$\begin{aligned} \phi &= \text{diag}\{e^{jkdsin\theta_1}, e^{jkdsin\theta_2}, \dots, e^{jkdsin\theta_D}\} \\ &= D \times D \text{ diagonal unitary matrix with phase shifts between doublets for each} \\ &\quad \text{DOA.} \end{aligned}$$

Creating the signal subspace for the two subarrays led the results in two matrices E_1 and E_2 . Since the arrays are translationally related, the subspaces of eigenvectors are related by a unique nonsingular transformation matrix Ψ such that

$$E_1 \Psi = E_2 \quad \text{equation (1.12)}$$

There must also exist a unique nonsingular transformation matrix T such that

$$E_1 = AT \quad \text{equation (1.13)}$$

and

$$E_2 = A\phi T \quad \text{equation (1.14)}$$

Substituting equation (1.12) and (1.13) into (1.14), we get

$$T \Psi T^{-1} = \phi$$

Thus, the eigenvalues of Ψ must be equal to the diagonal elements of ϕ such that

$$\lambda_1 = e^{jkdsin\theta_1}, \lambda_2 = e^{jkdsin\theta_2}, \dots, \lambda_D = e^{jkdsin\theta_D}$$

After the calculation of the eigenvalues of Ψ , $\lambda_1, \lambda_2, \dots, \lambda_D$, the angles of arrival can be estimated

as

$$\theta_i = \sin^{-1}(\arg(\lambda_i)/kd) \quad \text{equation (1.15)}$$

Roy et al. (1989) presented that ESPRIT reduces the computation complexity compared to other high resolution angle of arrival estimation algorithms as it doesn't search for the arrival angles for entire possible values of angle.

Dongarsane et al. (2011) analyzed the performance of ESPRIT algorithm with different parameters that plays important role in the estimation of DOA [35]. From their simulation result it can be observed that the percentage of error in DOA estimation decreases with increase in number of array elements in design as well as with increase in number of samples taken for the simulation. They also analyzed the algorithm by increasing the number of incoming signals keeping the number of array elements same. From this analysis they found out that the error in DOA estimation increases as the number of arriving signal increases. Also, percentage of error in DOA estimation increases as the difference between these arrival angles decreases.

Soon et al. (1992) analyzed the result of Mean Square Error (MSE) of ESPRIT and MUSIC and then also compared the result of one with the other [36]. From their simulation result, it was clear that the implementation of ESPRIT algorithm gives less MSE with maximum number of overlapping subarrays. From their result it can also be analyzed that MUSIC does have lower MSE than ESPRIT.

A.Abdallah et al. (2006) have proposed the design of smart antenna system with six port reflectometer that can detect angle of arrival for 5 signals [39]. Fig. 1.14 shows six port reflectometer's structure. Using this design, the response from MUSIC and ESPRIT algorithms were experimented for DOA estimation. For the simulation of design and implementation of these two algorithms, Advanced Design System (ADS) and MATLAB were respectively used.

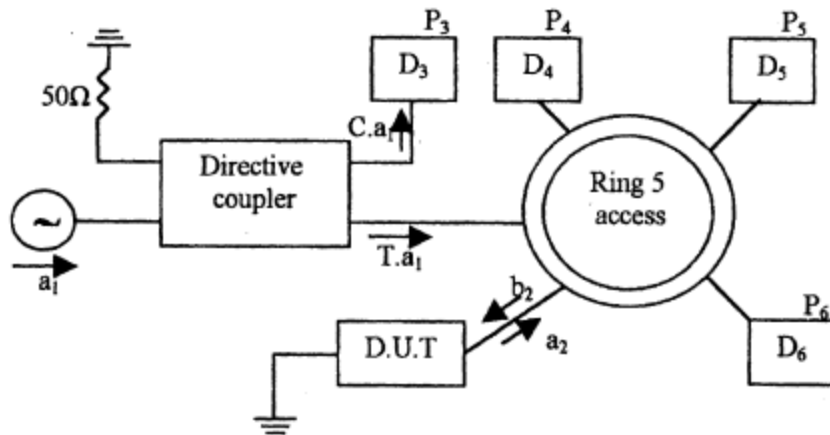


Figure 1.14: Reflectometer six ports [39]

In their experiment, hardware part was responsible for capturing the RF signals and then converting them into low frequency signals while software part detected this low frequency signals and did the estimation of arrival angles. The smart antenna circuit that includes antennas, low noise amplifiers (LNA) and six port junctions were calibrated to gather the necessary data for MUSIC and ESPRIT algorithms. With the enough data gathered from the hardware portion, the arrival angles were estimated using these two algorithms in MATLAB. As the result of simulation, responses of arrival angles from these two algorithms were presented. From their result it can be analyzed that MUSIC gives more accurate result for angle estimation than ESPRIT, and also accuracy from both of these algorithms increased with increase in SNR ratio. Though as it can be concluded that MUSIC have better accuracy than ESPRIT from their result, the parameters considered to get into this conclusion were not enough from their experiment. So there has to be more experiments done considering all the parameters that affects the angle estimation process.

T.B. Lavate et al. (2010) did simulation for performance analysis of MUSIC and ESPRIT using MATLAB [41]. They compared these two algorithms in terms of different parameters considering uniform linear array of antenna for the simulation.

Fig. 1.15 shows result from MUSIC algorithm for varying number of antenna elements, M . Here they have showed the power spectrum plot from MUSIC for number of antenna elements as 5 and 10. Similarly, fig. 1.16 shows result from MUSIC algorithm for varying number of samples, K . Here they have showed the power spectrum plot from MUSIC for number of samples as 10 and 100.

From T.B. Lavate et al. (2010) simulation's result for MUSIC and ESPRIT it can be analyzed that, as the number of antenna elements increases, accuracy for angle estimation also increases, and also it can be seen that the angular resolution was more accurate with the increase in the number of samples.

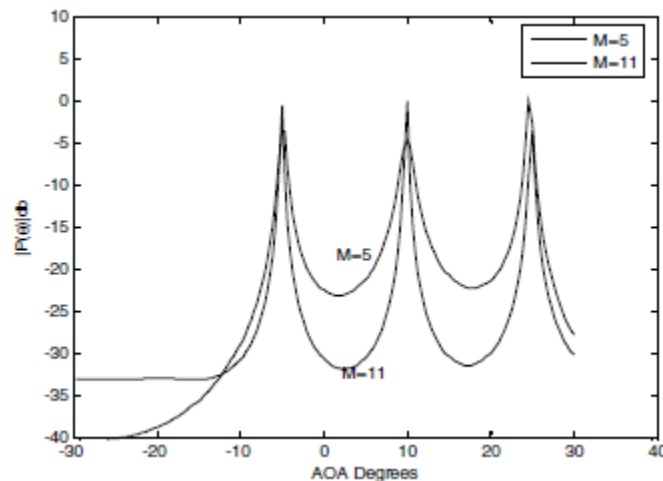


Figure 1.15: MUSIC spectrum for varying number of array elements [41]

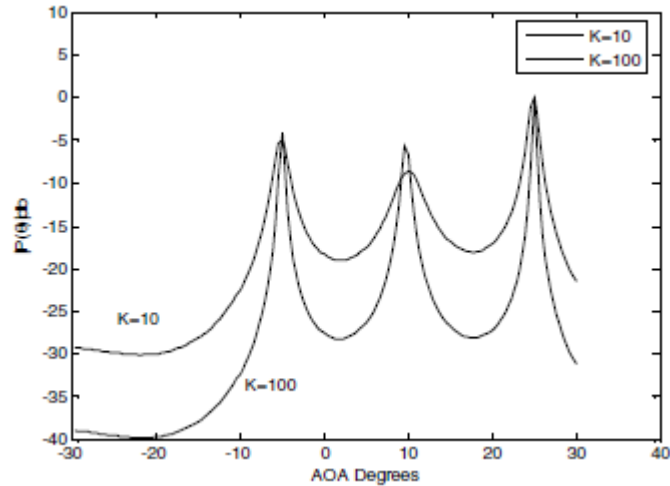


Figure 1.16: MUSIC spectrum for varying number of samples [41]

They also showed that, in case of ESPRIT as the number of arrival angle increases the accuracy in estimation of arrival angle decreases. For both of these algorithms, they showed that as the SNR increases, more précised result is obtained, though MUSIC has better resolution compared to the ESPRIT. Though both of these algorithms have high resolution for angle estimation, T.B. Lavate et al (2010) concluded MUSIC to be better than ESPIRIT as it has high resolution and more accuracy for the estimation of arrival angles. Though they concluded their experiment considering MUSIC to be best over ESPRIT, the parameters they considered for the analysis of these algorithms were not enough. There are other parameters need to be considered too, like angle difference between two signals, processing time of these two algorithm, etc.

1.6 Beamforming

After the knowledge of DOA of incoming signals, the next stage in the adaptive smart antenna system is beamforming. Fig. 1.17[16] shows the N-element array uniformly spaced in distance d .

The Array Factor (AF) for this array of antenna can be computed as

$$AF = 1 + e^{j(kd\cos\theta+\beta)} + e^{j2(kd\cos\theta+\beta)} + \dots + e^{j(N-1)(kd\cos\theta+\beta)}$$

where $k=2\pi/\lambda$, θ is the angle the signal and β is the phase shift between the elements

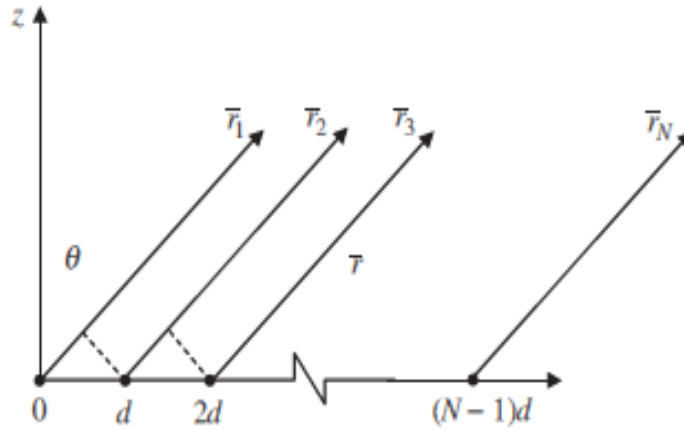


Figure 1.17: N-element linear array [16]

After the computation of the above equation AF is obtained as

$$AF = \frac{\sin(\frac{N}{2}\Psi)}{\frac{N}{2}\Psi} \quad \text{equation (1.16)}$$

where $\Psi=kdcos\theta+\beta$

To steer the beam in the direction of the desired signal θ_0 , the phase shift, $\beta= -kdcos\theta_0$ as maximum value can be gained when $\Psi=0$ in the above equation.

The value of phase constant should be changed when beam has to be steered in the other direction. This enhances the SINR of the system as beam is being steered in the direction of the user. Though the beam is steered in the desired direction, still the interfering signal should be nullified.

To nullify the interfering signal the complex weight of the signal should be computed in such a way that it maximizes the beam in the desired direction and nullifies in the direction of interferer.

So weighing of the signal with the appropriate weight itself can steer the beam in the desired direction as well as nullifies the interferers.

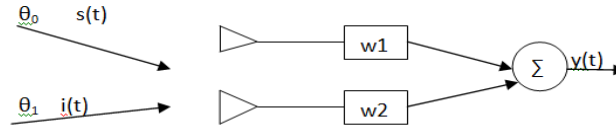


Figure 1.18: Two element array with desired and interfering signals

For the two element array shown in fig. 1.18, θ_0 and θ_1 are the angle of desired signal, $s(t)$ and interfering signal, $i(t)$ respectively. If w_1 and w_2 are the weights for the signal through first and second elements respectively, then the output y_1 and y_2 due to two different signals $s(t)$ and $i(t)$ respectively can be computed as

$$y_1 = w_1 e^{j(kd \cos \theta_0)} + w_2 e^{j(kd \cos \theta_0)} = 1 \quad \text{equation (1.17)}$$

$$y_2 = w_1 e^{j(kd \cos \theta_1)} + w_2 e^{j(kd \cos \theta_1)} = 0 \quad \text{equation (1.18)}$$

In equation (1.17), the output y_1 is made equal to 1 as it is the output from the desired signal which should be maximized, and in equation (1.18), the output y_2 from the interfering signal is made 0 so that the beam pattern can be nullified in the interferer direction. When the weights w_1 and w_2 obtained from the above two equations are applied to the received signals the radiation beam is steered in the desired direction and nullified in the direction of interferer.

This technique of beamforming is only necessary for DOA-based adaptive beamforming algorithms. For reference (or training) based adaptive beamforming algorithms, the adaptive beamforming algorithm does not need the DOA information but instead uses the reference

signal, or training sequence, to adjust the magnitudes and phases of each weight to match the time delays created by the impinging signals into the array [4]. This technique of beamforming is also known as optimized beamforming. Some of the algorithms that implements this technique are Least Mean Square (LMS), Sample Matrix Inversion (SMI), Recursive Least Squares (RLS), Constant Modulus Algorithm(CMA), conjugate gradient and waveform diverse algorithm.

The basic principle of these algorithms is to find out the error which is the difference between the desired signal or also known as trained signal and the output signal. And these different algorithms have different techniques through which they try to minimize this error so that the output signal matches the desired signal. These algorithms are also capable to keep track of the change of the direction of desired user.

Rani et al. (2007), presented DOA estimation using MUSIC algorithm and LMS for the beamforming [43]. For LMS algorithm they calculated the error signal which gave difference between the training or the desired signal and the complex weight vector. The complex weight vector was adaptively adjusted to give the least mean square error. With the minimum mean square error, the complex weight vector computed locked the beam of radiation pattern in the direction of the desired signal and nullified in the direction of interfering signals. They also showed that with the increase in number of elements, better beam pattern can be obtained.

1.7 Hardware implementation for smart antenna

Hou et al(2009) have designed and implemented a real-time DOA estimation system using TMS320VC33 processor chip as a core processor, AD7891 chip as analog-to-digital converter, and the associated hardware circuits [45]. Fig. 1.19 shows the block diagram of real-time DOA estimator VC33 prototype system of Hou et al (2009). They tested the prototype system via computer simulation and conducted experiments in the shallow water.

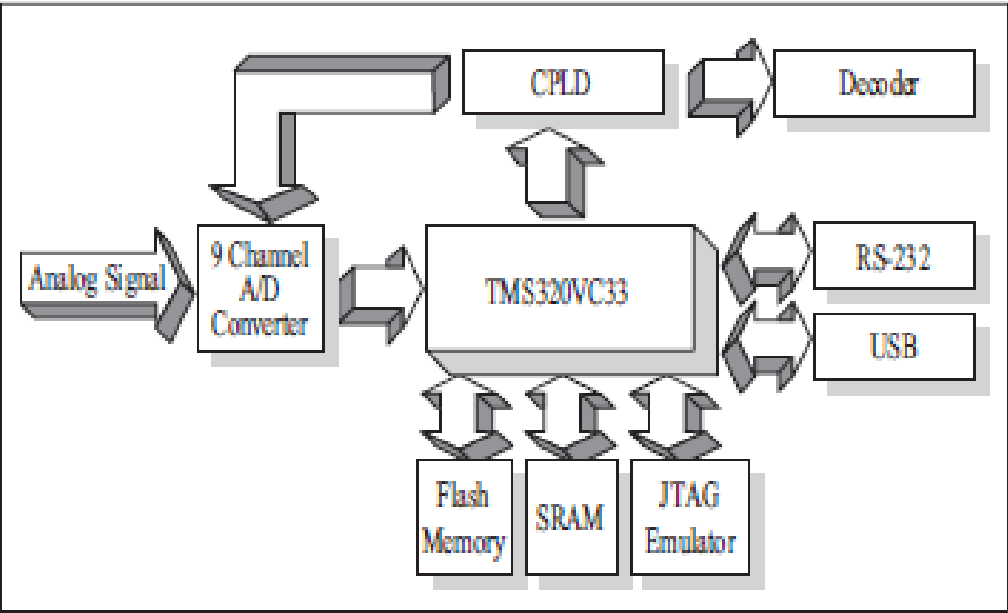


Figure 1.19: Block diagram of real-time DOA estimator VC33 prototype system [45]



Figure 1.20: Equipment setup at transmitter site [45]



Figure 1.21: Equipment setup at receiver site [45]

Hou et al (2009) experimented MUSIC, Reduced Order Root MUSIC (RORM), Spatial Smoothing MUSIC (SSM) and Least Squares (LS) in their experimental set up. These algorithms were coded so they get executable by the lab-view system as well as its associated hardware. Fig. 1.20 and 1.21 shows the equipment setup at transmitter and receiver site of their experiment respectively. The TMS320VC33 processor they used played a central role for data retrieval and program execution. AD7891 chip was used to transform analog acoustic signals into digital codes. IDT-71V242-10 SRAM and AT29LV040A-150 flash memory were used for data/program storage and retrieval and CPLD was incorporated for convenient and flexible design of decoder device.

Hou et al (2009) confirmed that their experiment on VC33 incorporated with a receiving hydrophone array and associated devices can form a prototype system suitable for estimating multiple underwater acoustic sources. They also assured that the complete prototype is able to locate the directions of underwater acoustic sources in real time.

Hua et al (2012) used software defined radio (SDR) platform to estimate DOA of signals [46]. Fig. 1.22 shows the picture of SDR platform they used. The SDR platform includes four independent RF receivers, an analog-to-digital converter (ADC) and a signal processing module is used to implement a real-time DOA estimator. This DOA estimator was tested in a microwave anechoic chamber.

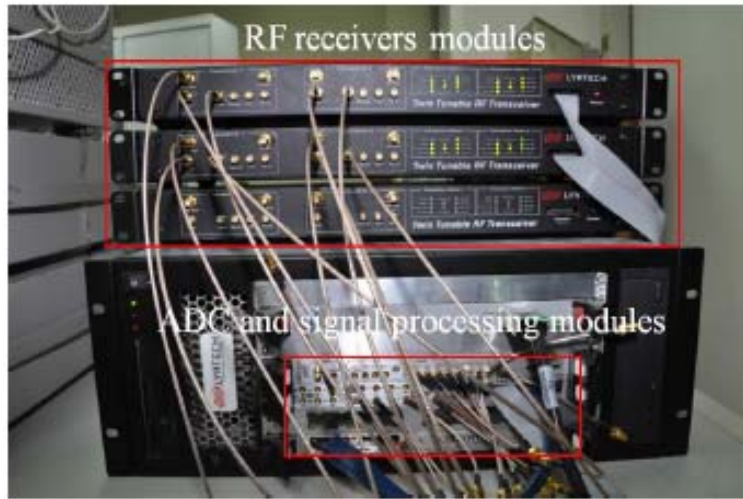


Figure 1.22: Photograph of SDR platform [46]

Fig. 1.23 shows the block diagram of hardware configuration of Hua et al (2012) system.

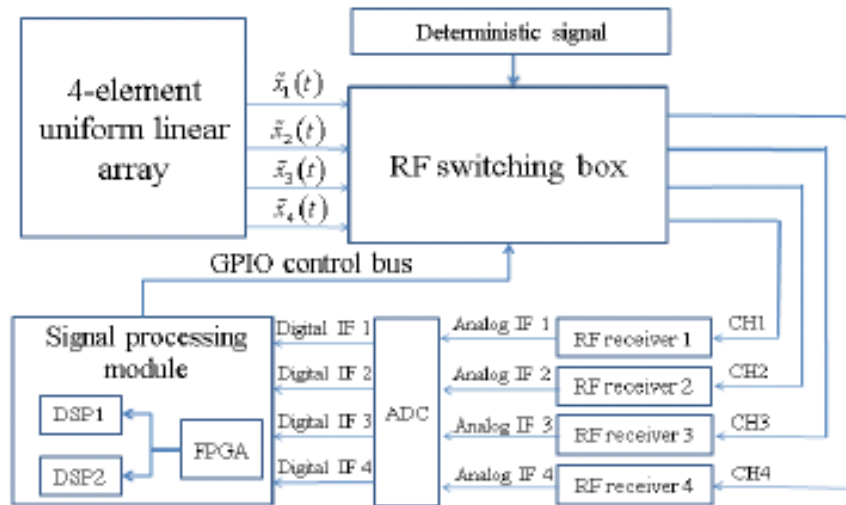


Figure 1.23: Block diagram of hardware configuration [46]

The RF receiver modules of Hua et al (2012) employed a super heterodyne architecture which converted RF input signals to a 30MHz intermediate frequency (IF) analog signals. A subsequent high speed ADC module with maximum sampling rate of 105MHz digitized the IF analog signal. The digitized data was sent to a signal processing module, which comprised one Virtex-4 FPGA and two TMS320C6416 DSPs. They also designed FPGA to convert the digitized IF data into baseband data. They used one DSP to perform phase calibration of RF receivers and the other was used to execute DOA estimation algorithms based on the collected data. The DOA algorithm they used for their experiment was MUSIC. The signal processing module controlled RF switching box via General Purpose Input/ Output (GPIO) interface. The results for spatial spectrum and DOA estimation were displayed on the host PC.

Hua et al confirmed that the experimental results from anechoic chamber showed that the system was able to detect the number of source and also the directions of incoming signals in real time.

Wang et.al (2006) designed a smart antenna system that combines technologies of antenna design, signal processing, and hardware implementation [47]. In their system, after the digital signal processor receives the signals collected from each antenna element, it computes the direction of arrival of all incoming signals.

Fig. 1.24 shows the structure of the receiver of Wang et.al (2006) system. They have used 4-element linear antenna array to receive signals. The received signals are then converted from 10 GHz frequency to the intermediate frequency 71 MHz and finally through I/Q demodulation to the baseband. After A/D conversion, the measured data were used for DOA analysis through PC. Then further of the signal processing to estimate DOA was done in FPGA. The required input for FPGA like number of antenna elements, number of incoming signals and their respective angles

were sent from PC. They used Xilinx XC2VP30 as the FPGA device. The estimated DOAs from their lab setup using MUSIC algorithm was very close to real DOAs and the total time consumed for processing was also less than 30 μ s.

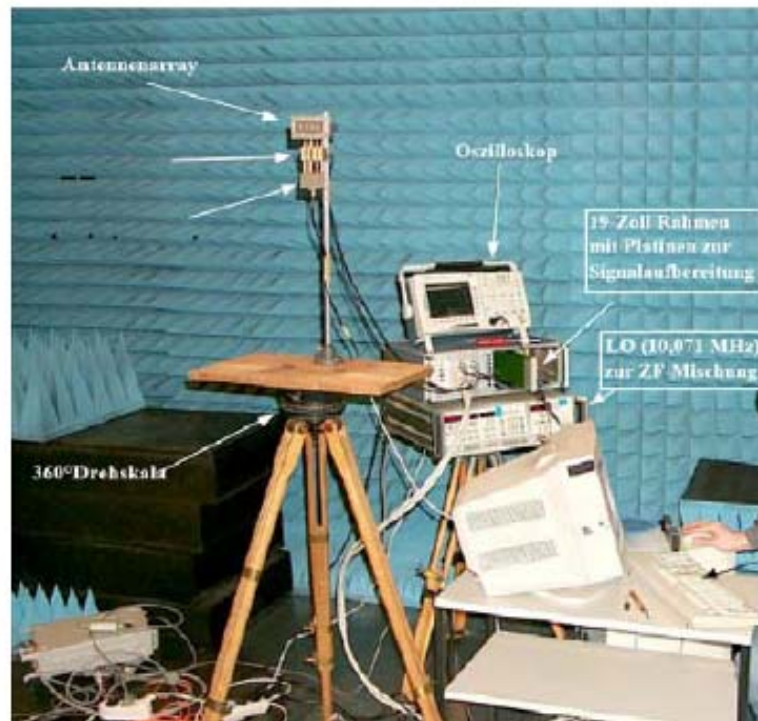


Figure 1.24: Structure of the receiver [47]

1.8 Summary

The evolution of smart antenna system started with the cellular concept in mobile communication. To increase the capacity of channels, concepts of cell splitting and cell sectoring emerged. With the increasing demand for higher wireless communication bandwidth, these methods were not able to meet those demands. Hence, the new technology of smart antenna was developed to cope with these increasing demands. This technology is based on switched beam system and adaptive beam system. Adaptive beam system is superior to switched beam system as it is capable to totally reject the interfering signals. Usually adaptive beam system has two

stages; DOA estimation and then adaptive beamforming. There are many algorithms developed till this date for both DOA estimation and for adaptive beamforming.

Hence, in this chapter, detail study of some DOA estimation algorithms like MUSIC and ESPRIT was done with some other algorithms. Also the technique of beamforming was discussed in detail with the mention of some of the adaptive beamforming algorithms.

CHAPTER II

METHODOLOGY

Direction of Arrival (DOA) estimation plays an important role in a smart antenna. Algorithms to determine DOA are responsible for estimating the angles of arrival of the signals impinging on the smart antenna accurately and efficiently. The information obtained by the DOA stage is passed to the 'Beamforming' stage in order to modify the radiation pattern of the antenna. This modification implies to orientate the main beam in the direction of the desired users and the nulls in the direction of the interferers.

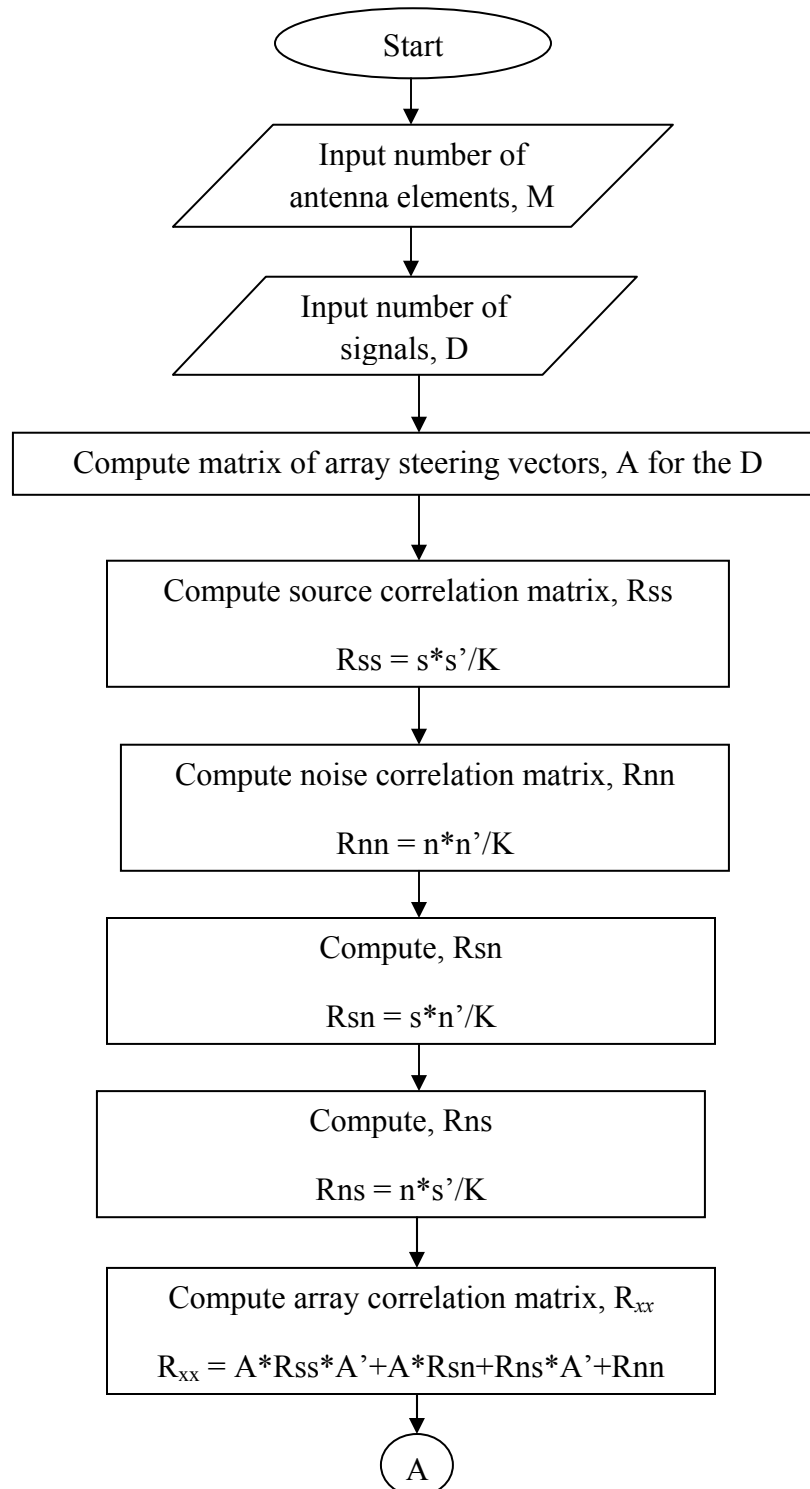
This chapter includes the methodology of implementation of MUSIC and ESPRIT algorithms. In successful design of an adaptive array smart antenna system, the performance of DOA algorithms highly depends on many parameters such as number of array elements, number of users and space distribution between them, spacing between the array elements, number of signal samples and SNR. This chapter includes detail of all the methods implemented for the study of these parameters with MUSIC and ESPRIT algorithms.

2.1 MUSIC Algorithm

The study of MUSIC algorithm was done with MATLAB and Simulink. This algorithm was coded in MATLAB first and later it was implemented in Simulink. In Simulink the algorithm was coded in MATLAB along with the use of other functional block for the signal and noise

generation. Flowchart for MUSIC algorithm is followed after this, on the basis of which the algorithm was coded in MATLAB.

2.1.1 Flowchart for MUSIC



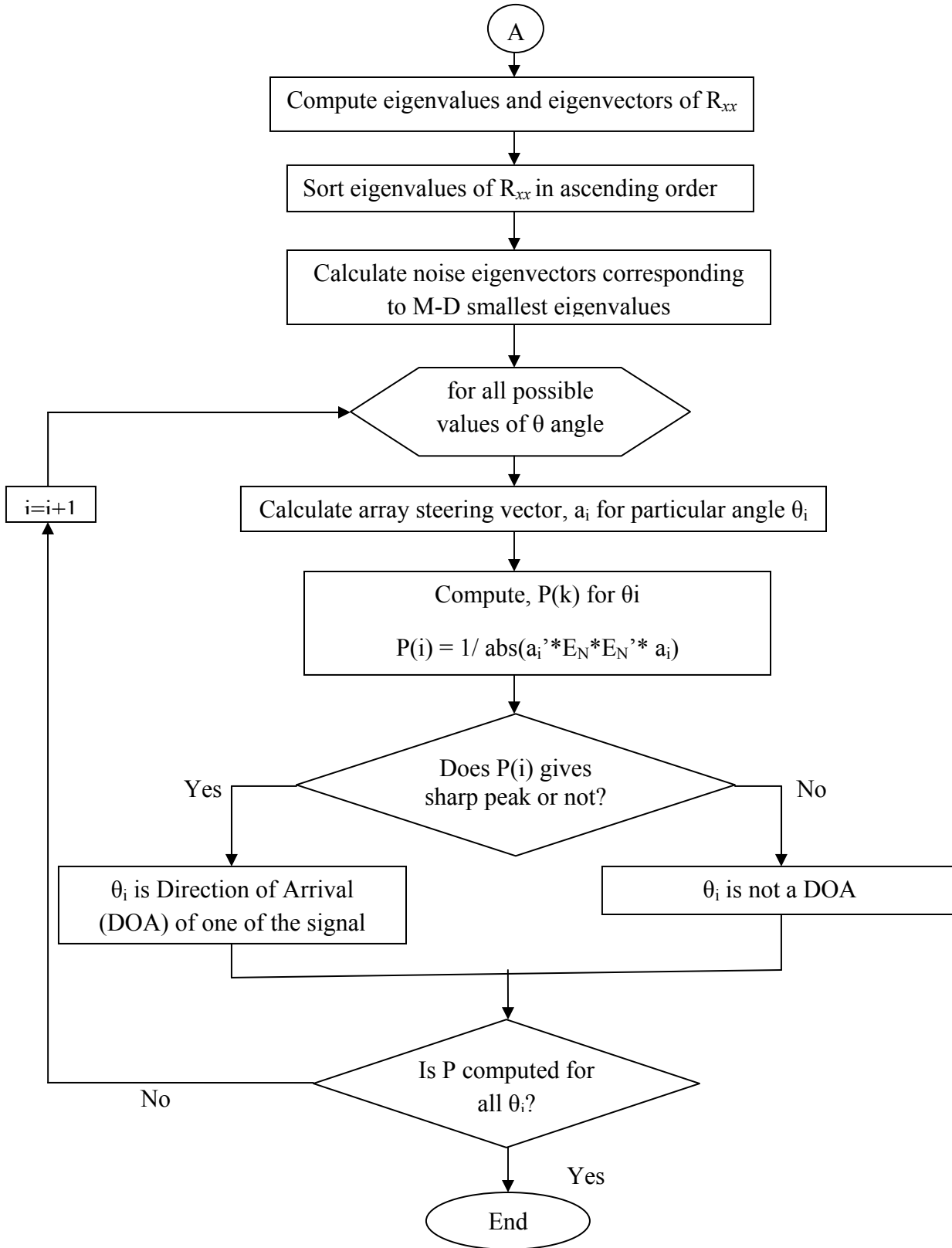
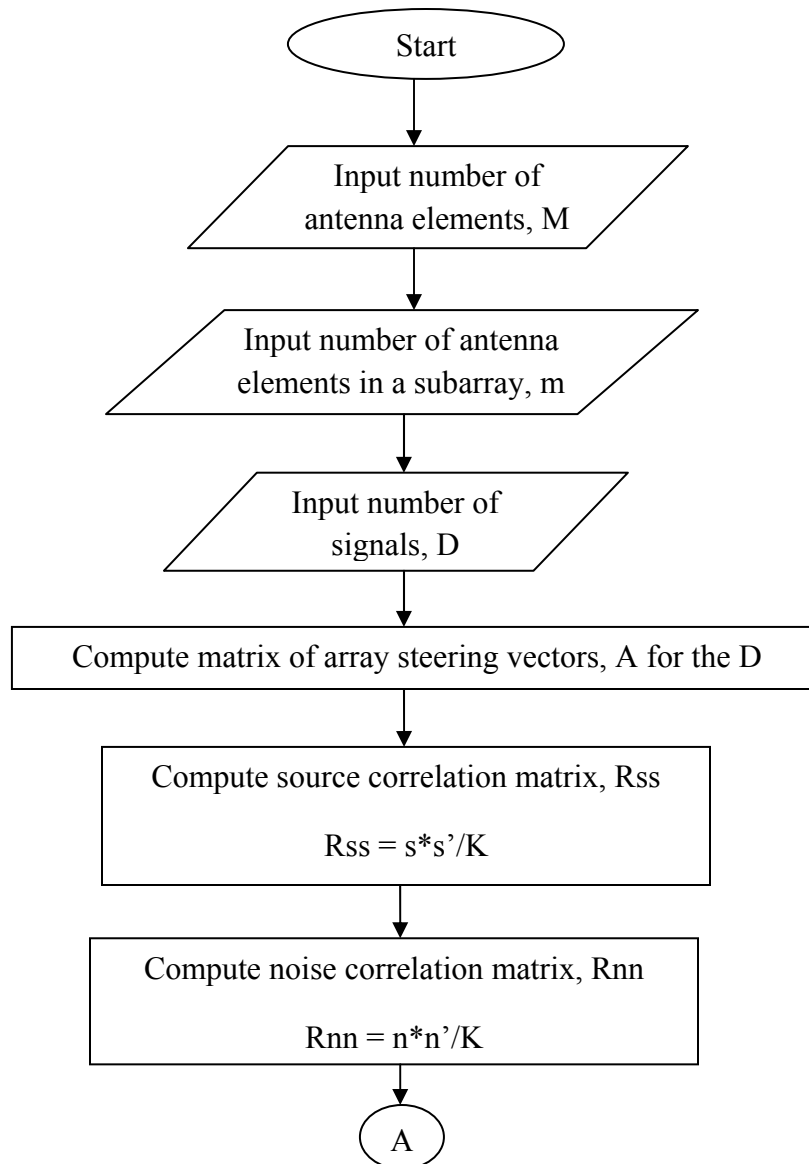


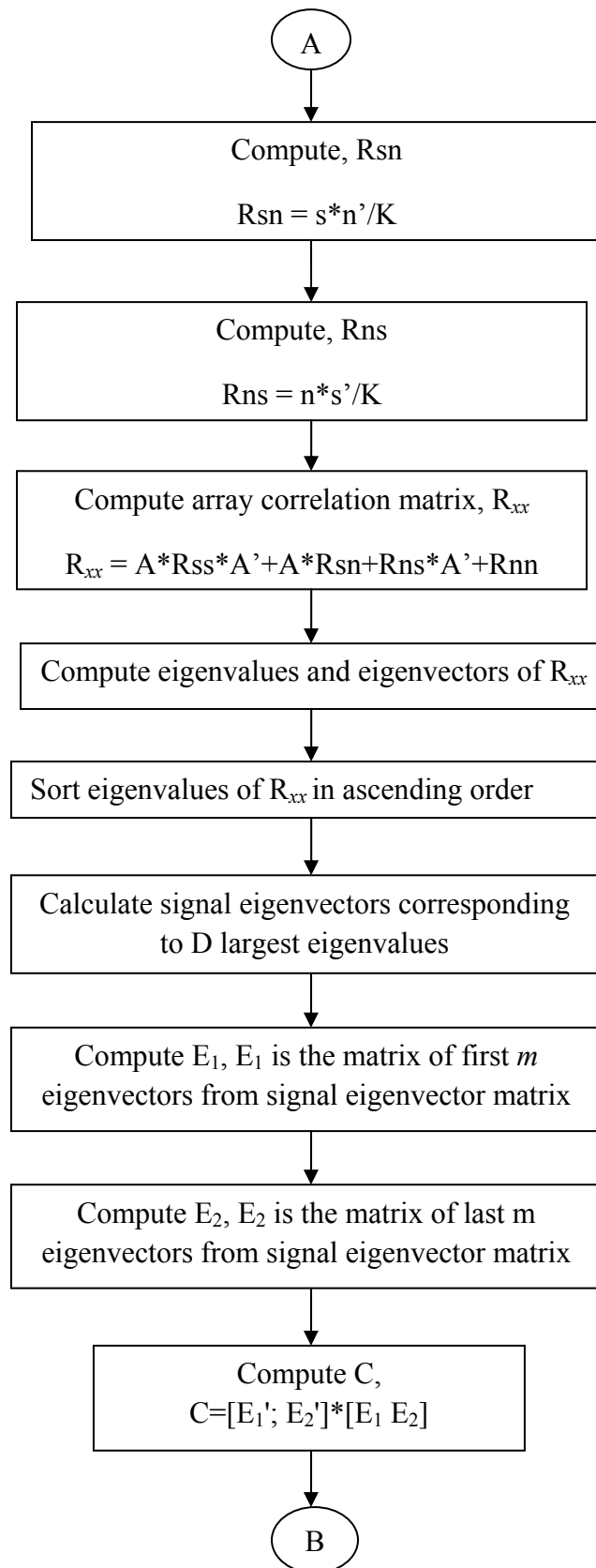
Figure 2.1: Flowchart of MUSIC algorithm

2.2 ESPRIT Algorithm

The study of ESPRIT algorithm was done with MATLAB and Simulink. This algorithm was coded in MATLAB first and later it was implemented in Simulink. In Simulink this algorithm was coded in MATLAB along with the use of other functional block for the signal and noise generation. Flowchart for ESPRIT algorithm is shown below, on the basis of which this algorithm was coded in MATLAB.

2.2.1 Flowchart for ESPRIT





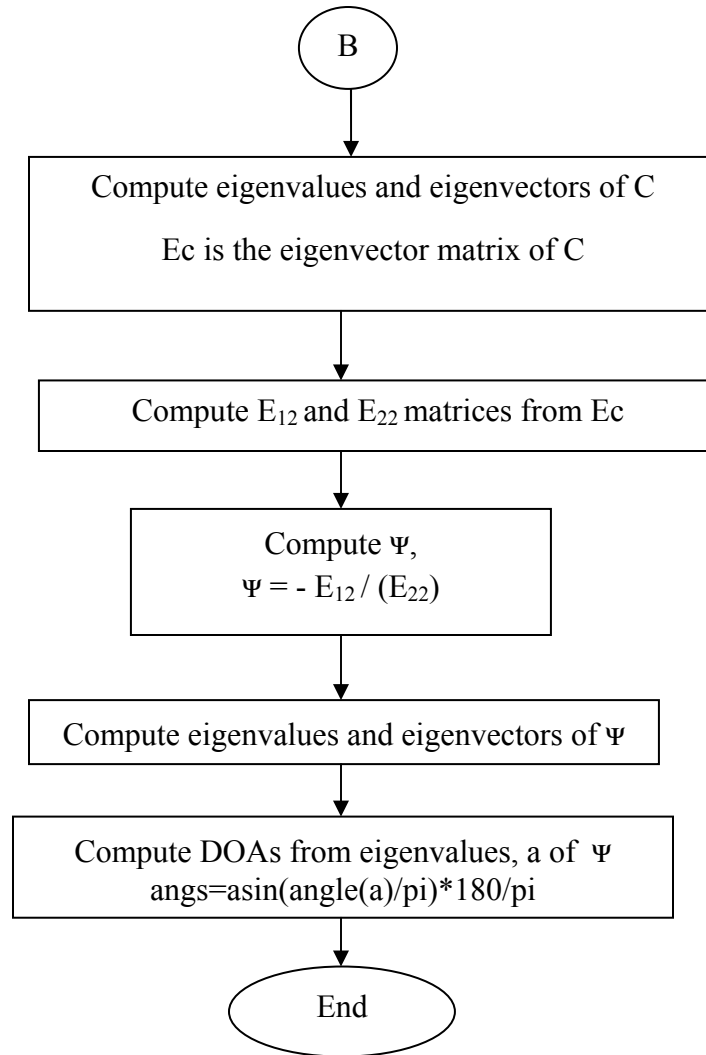


Figure 2.2: Flowchart of ESPRIT algorithm

Study and comparison between MUSIC and ESPRIT algorithm were done with MATLAB and Simulink. Simulation of these algorithms were done on the basis of different parameters like number of antenna elements, number of signals, number of signal samples, difference between angles of two signals and SNR ratio to test the performance of these algorithms. The methodology of implementation of these algorithms using MATLAB and Simulink is described below in detail.

2.3 Methodology for MATLAB

Coding was done for the analysis of MUSIC and ESPRIT algorithm in MATLAB. The coding for MUSIC in MATLAB was done on the basis of flowchart for MUSIC algorithm in fig. 2.1 and for ESPRIT, coding was done in the basis of flowchart for ESPRIT algorithm in fig.2.2.

For MUSIC, result was obtained through the power spectrum plot from the program. The angles which have the peak values in the power spectrum plot were the estimated angles for the incoming signals impinging to the array of antenna. While for ESPRIT, results were displayed in the command window.

2.3.1 Functions that were used while coding MUSIC and ESPRIT algorithms

randn(m,n) : Returns $m \times n$ matrix of normally distributed pseudorandom numbers. This function was used to generate n times samples of the signal for m number of arriving signals. It was also used to generate n times samples of the noise for m number of array elements.

mean(A) : Returns the mean value or average value of a vector A . This function was used to calculate power of signal as well as of noise to determine SNR ratio.

eig(A) : Returns eigenvalues and eigenvectors of matrix A . This function was used to compute eigenvalues and eigenvectors of array correlation matrix in both MUSIC and ESPRIT. It was also used to calculate eigenvalues and eigenvectors of rotation operator in ESPRIT.

sort() : Sort elements of array in ascending or descending order. It was used to sort the calculated eigenvalues of array correlation matrix from least to greatest.

clear : clears variables and items from current workspace, releasing them from system memory. It was used to clear variables from system memory as those variables were used repeatedly in the program code.

exp() : This is an exponential function. It was used to calculate array steering vector in both of the algorithms.

abs(A) : Returns the absolute values of A. A can be a variable or constant or an array. If A is an array, **abs()** function returns an array with its element having absolute value of each corresponding element of A. It was used to calculate the power spectrum in MUSIC algorithm.

sqrt(A) : Returns the square root of A. It was used to calculate square root of a constant.

sin() : Returns the sin of the argument in radians. It was used for the computation of array steering vector.

max(A) : If A is a vector, returns the largest element in A. It was used to find out the maximum value of power spectrum for the normalized power spectrum plot of MUSIC.

for loop : It is a loop that executes the statement within the loop repeatedly until the value of a variable reaches the finish value. It was used to compute the value of power spectrum for each possible angle.

if : Is a conditional statement. Statements within this conditional statement are executed only if the condition of this conditional statement is true. This was used to verify if the signal received is in the range of particular antenna element from array or not.

plot(X,Y) : Plots each vector Y versus each vector X on the same axes. It was used for the power spectrum plot in MUSIC.

tic, toc : tic starts the stopwatch timer while toc stops the stopwatch timer started by tic. toc function displays the elapsed time since the most recent tic. tic function was used at the beginning of the MATLAB code and toc at the end of the code for both MUSIC and ESPRIT to measure the elapsed time between beginning and end of the program.

grid : Grid lines for 2-D and 3-D plots. It was used as function 'grid on'. 'grid on' adds major grid lines to the current axes.

xlabel : Labels the x-axis of the current axes. It was used to label the x-axis of power spectrum plot in MUSIC.

ylabel : Labels the y-axis of the current axes. It was used to label the y-axis of power spectrum plot from MUSIC.

axis ([xmin xmax ymin ymax]) : Sets the limit for the x- and y-axis of the current axes. It was used to set the limit of x- and y- axis of power spectrum plot from MUSIC.

2.4 Methodology for Simulink

Simulink is a block diagram environment for modeling, simulating, analyzing multidomain dynamic systems. It has set of block libraries. It can provide good integration with MATLAB environment, and also it can even drive MATLAB or be scripted through it.

For the simulation in Simulink, interfacing between different blocks and MATLAB code was done through MATLAB function block. Signals were generated through random source block and noise from gaussian noise generator. The signals and noise generated were send as inputs for the MATLAB function block, and rest of the processing was done in this function block.

2.4.1 Block diagram for MUSIC algorithm in Simulink

Fig. 2.3 shows the block diagram for MATLAB in Simulink. Here four random sources are used to generate four different incoming signals. Each random source generates a signal with K number of samples. Similarly, Gaussian noise generator generates noise for M number of antenna elements with each having K samples i.e. it will generate a noise with $M \times K$ matrix size, where M is the number of antenna elements in antenna array and K is the number of samples. Here, sign blocks, transpose blocks, divide block, constant block and sqrt block are used to conduct different operations over signal and noise matrices. Later in this chapter each of these block will be explained in detail.

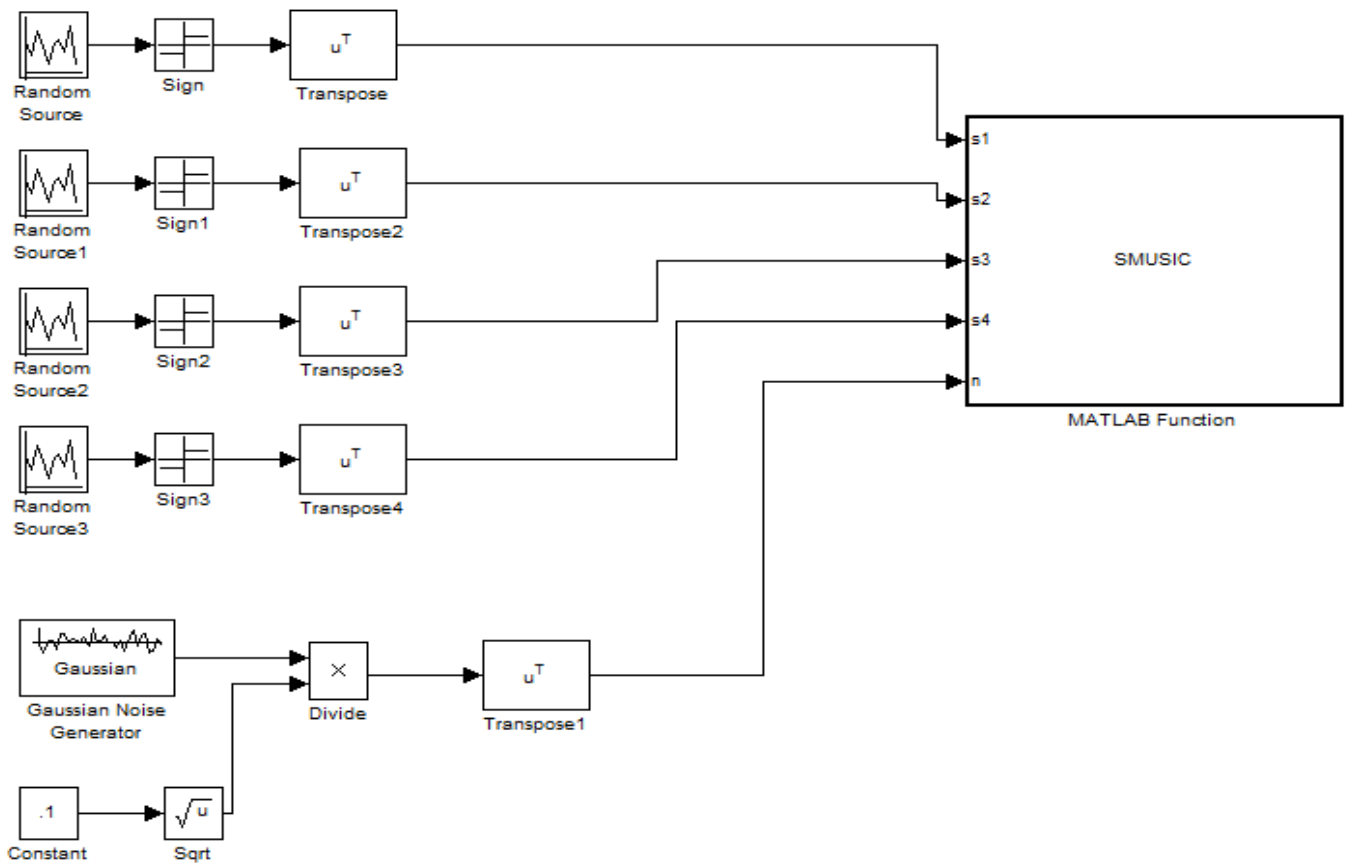


Figure 2.3: Block diagram for MUSIC algorithm in Simulink

In fig. 2.3 MATLAB function block takes all signals with K samples and noise with M X K dimension as the input. It does rest of the processing for the MUSIC algorithm through MATLAB's code. Plot generated from MATLAB function block was used for the angle estimation of arrival signals.

2.4.2 Block diagram for ESPRIT algorithm in Simulink

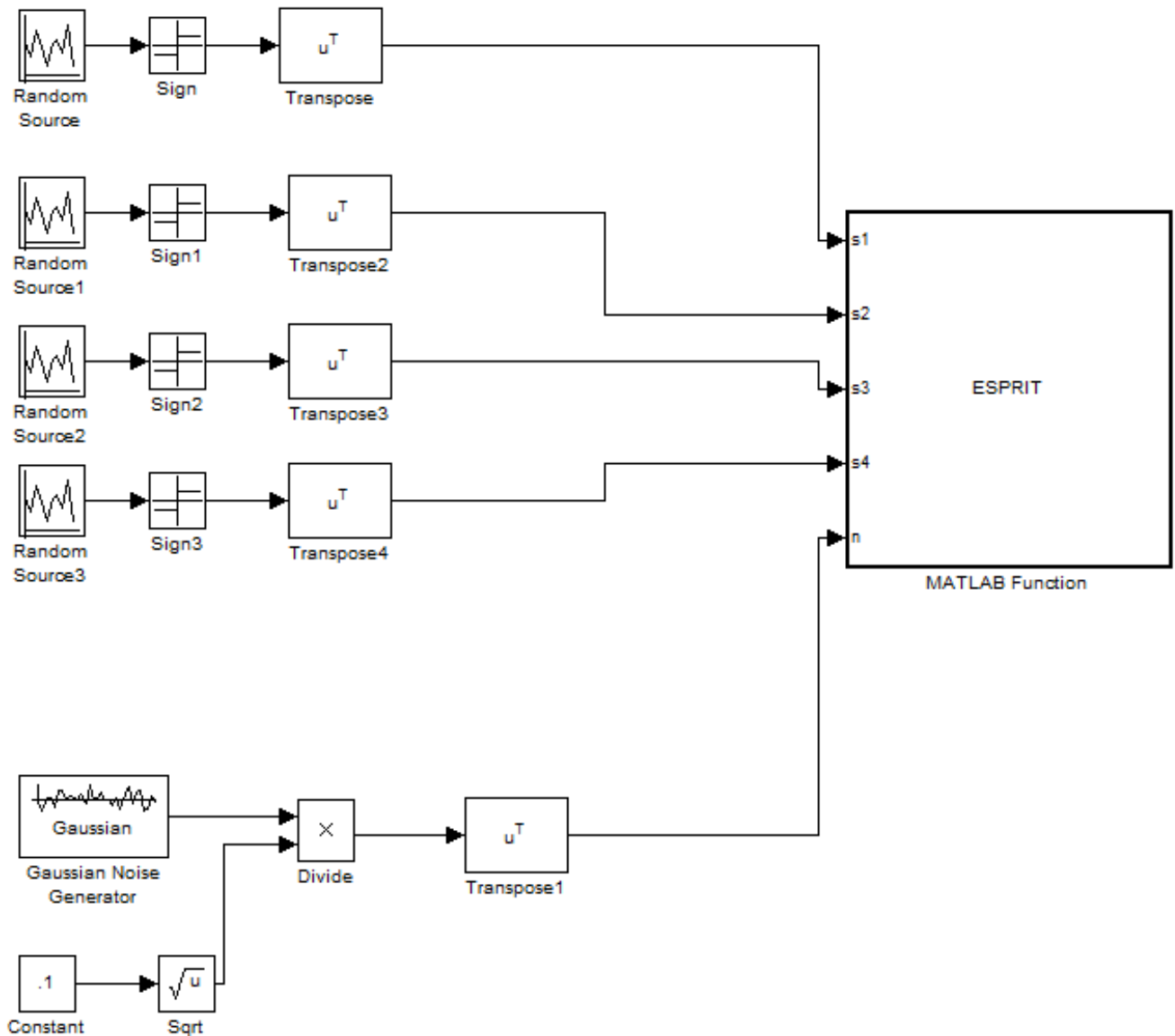


Figure 2.4: Block diagram for ESPRIT algorithm in Simulink

Fig. 2.4 shows the block diagram of ESPRIT algorithm in Simulink. Blocks used for ESPRIT in Simulink is same as that of MUSIC. All of them perform same operations as described in above section of MUSIC algorithm's block diagram except MATLAB function block. In case of ESPRIT, MATLAB function block is programed for ESPRIT algorithm, and results of angle estimation are displayed in command window.

2.4.3 Blocks that were used for MUSIC and ESPRIT algorithms in Simulink

Simulink software package was taken as reference to explain these blocks with their parameters.

2.4.3.1 Random source

For the access of Random Source block in Simulink, it should be proceeded with following flow: Simulation Processing Blockset -> Blocks -> Signal Processing Sources -> Random source.



Figure 2.5: Random Source Block

The Random Source block generates a frame of K values drawn from a uniform or Gaussian pseudorandom distribution, where K is specified in the **Samples per frame** parameter.

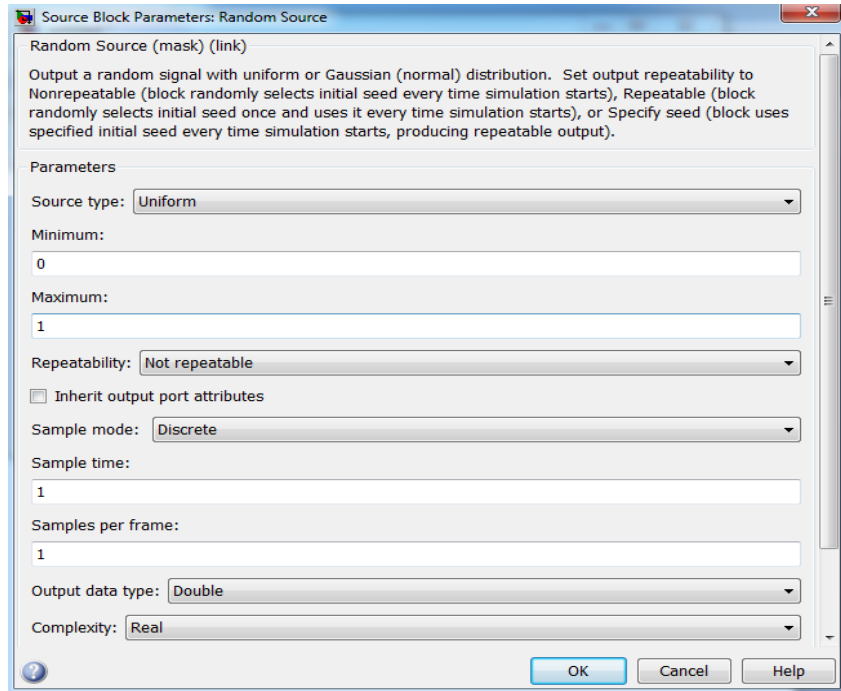


Figure 2.6: Dialog box of Random Source

Parameters for random source block:

Source type: The distribution from which to draw the random values, *Uniform* or *Gaussian*.

Minimum: The minimum value in the uniform distribution. This parameter is enabled when *Uniform* is selected from the **Source type** parameter.

Maximum: The maximum value in the uniform distribution. This parameter is enabled when *Uniform* is selected from the **Source type** parameter.

Initial seed: The initial seed(s) is used for the generation of random number. **Repeatability** parameter has to be set to *Specify seed* to input **Initial seed**.

Inherit output port attributes: When this check box is selected, block inherits the sample mode, sample time, output data type, complexity, and signal dimensions of a sample-based signal from a downstream block. When this check box is selected, the **Sample mode**, **Sample time**, **Samples per frame**, **Output data type**, and **Complexity** parameters are disabled.

Sample mode: The sample mode, *Continuous* or *Discrete*.

Sample time: The sample period, T_s , of the random output sequence. The output frame period is $K \cdot T_s$, where K is the samples per frame.

Samples per frame: The number of samples, K , in each output frame. When the value of this parameter is 1, the block outputs a sample-based signal.

Output data type: The data type of the output, *single-precision* or *double-precision*.

Complexity: The complexity of the output, *Real* or *Complex*.

2.4.3.2 Gaussian Noise Generator

For the access of Gaussian Noise Generator block in Simulink, it should be proceeded with following flow:

Communications Blockset -> Blocks -> Communication Sources -> Noise Generators -> Gaussian Noise Generator.



Figure 2.7: Gaussian Noise Generator Block

Gaussian noise generator generates Gaussian distributed noise with given mean and variance values. The Gaussian Noise Generator block generates discrete-time white Gaussian noise.

Initial seed vector must be specified in the simulation.

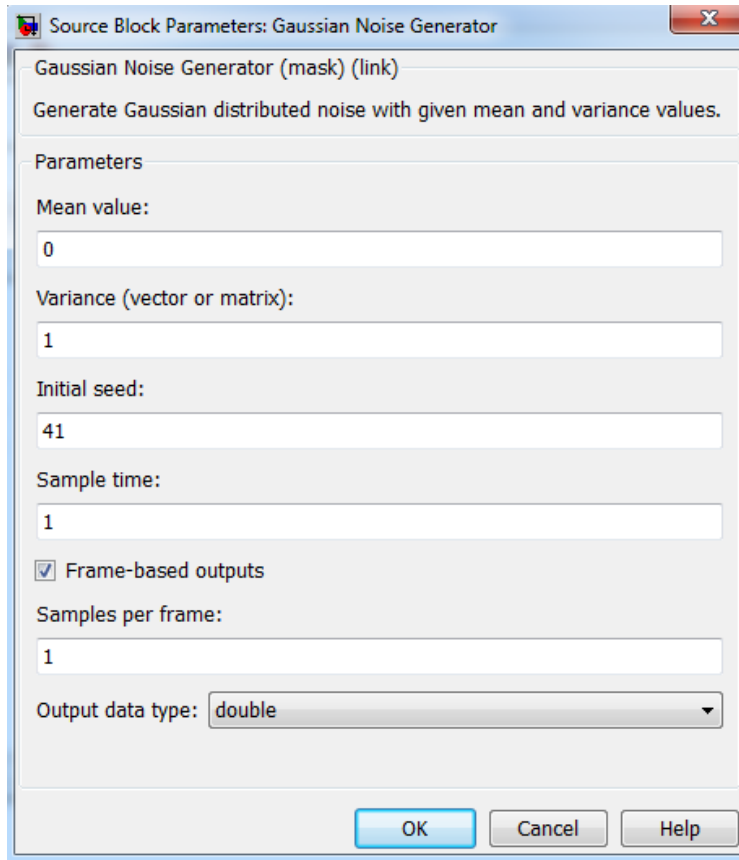


Figure 2.8: Dialog box of Gaussian Noise Generator

Parameters for Gaussian noise generator block:

Mean value: The mean value of the random variable output.

Variance: The covariance among the output random variables.

Initial seed: The initial seed value for the generation of random number.

Sample time: The period of each sample-based vector or each row of a frame-based matrix.

Frame-based outputs: Determines whether the output is frame-based or sample-based. This box is active only if **Interpret vector parameters as 1-D** is unchecked.

Samples per frame: The number of samples in each column of a frame-based output signal.

This field is active only if **Frame-based outputs** is checked.

Interpret vector parameters as 1-D: If this box is checked, then the output is a one-dimensional signal. Otherwise, the output is a two-dimensional signal. This box is active only if

Frame-based outputs is unchecked.

Output data type: The output can be set to *double* or *single* data types.

2.4.3.3 MATLAB Function block

For the access of MATLAB Function block in Simulink, it should be proceeded with following flow:

Simulink -> Blocks -> User-Defined Functions -> MATLAB Function.

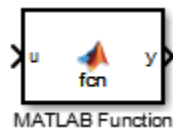


Figure 2.9: MATLAB Function Block

With a MATLAB Function block, MATLAB function can be written in Simulink model. It allows to add MATLAB functions to Simulink models for deployment to desktop and embedded processors. This capability is useful for coding algorithms that can be better stated in the textual language of the MATLAB software than in the graphical language of the Simulink product.

Fig. 2.10 shows the MATLAB function block's editor window where MATLAB function can be written. In above window, example to calculate mean of a vector, v is shown. Input for this function is v and output is y , and name of this function to calculate mean is `fcn`.

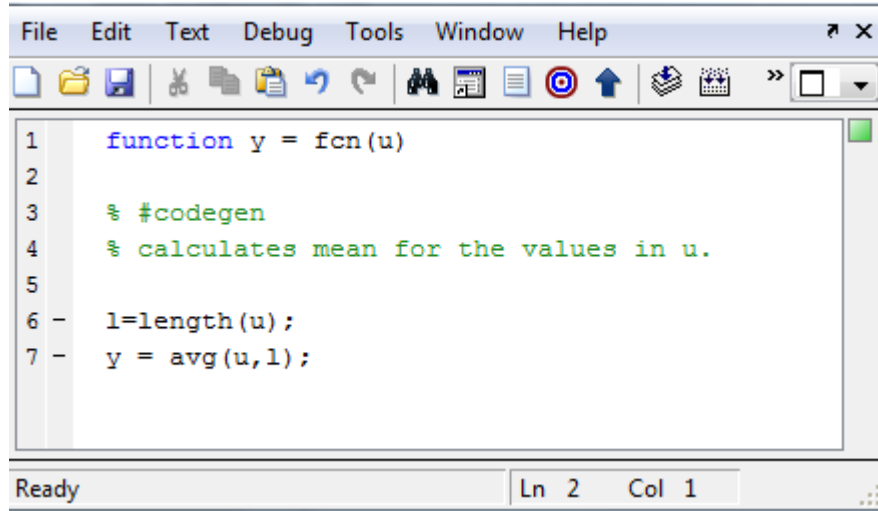


Figure 2.10: Editor for MATLAB Function block

Hence in MATLAB functional block, coding of the algorithms can be done along with the interaction with various Simulink blocks.

2.4.3.4 Transpose

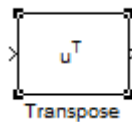


Figure 2.11: Transpose Block

For the access of Transpose block in Simulink, it should be proceeded with following flow:
Simulation Processing Blockset -> Blocks -> Math Functions -> Matrices and Linear Algebra -> Matrix Operations -> Transpose.

Transpose block transposes the matrix.

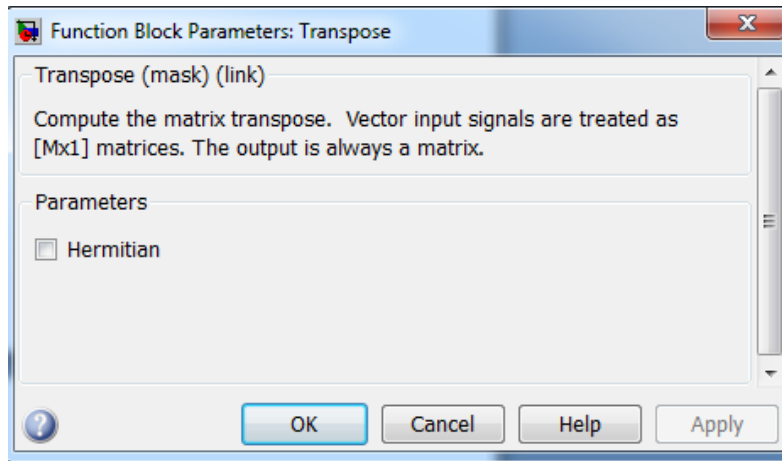


Figure 2.12: Dialog box of Transpose

Parameter of transpose block:

Hermitian: When it is checked, it specifies complex conjugate transpose.

2.4.3.5 Sign

For the access of Sign block in Simulink, it should be proceeded with following flow:

Simulink -> Blocks -> Math Operations -> Sign.

It indicates sign of the input. Gives 1 as output when input is greater than 0, 0 when input is 0 and -1 when input is less than 0.



Figure 2.13: Sign Block

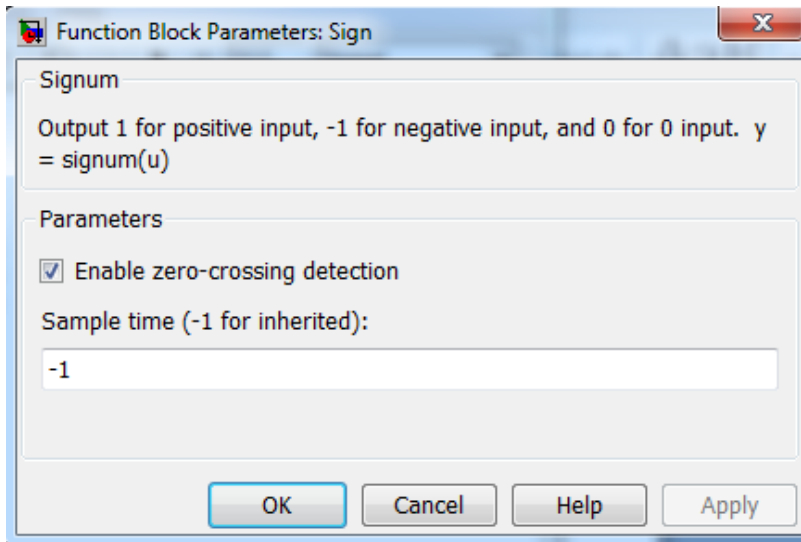


Figure 2.14: Dialog box of Sign

Parameters of sign block:

Enable zero-crossing detection: It is selected to enable zero-crossing detection.

Sample time (-1 for inherited): Specify the time interval between samples. To inherit the sample time, this parameter is set to -1.

2.4.3.6 Product

For the access of Product block in Simulink, it should be proceeded with following flow:
Simulink -> Blocks -> Commonly Used -> Product.

It multiplies and divides scalars and nonscalars or multiplies and invert matrices.



Figure 2.15: Product Block

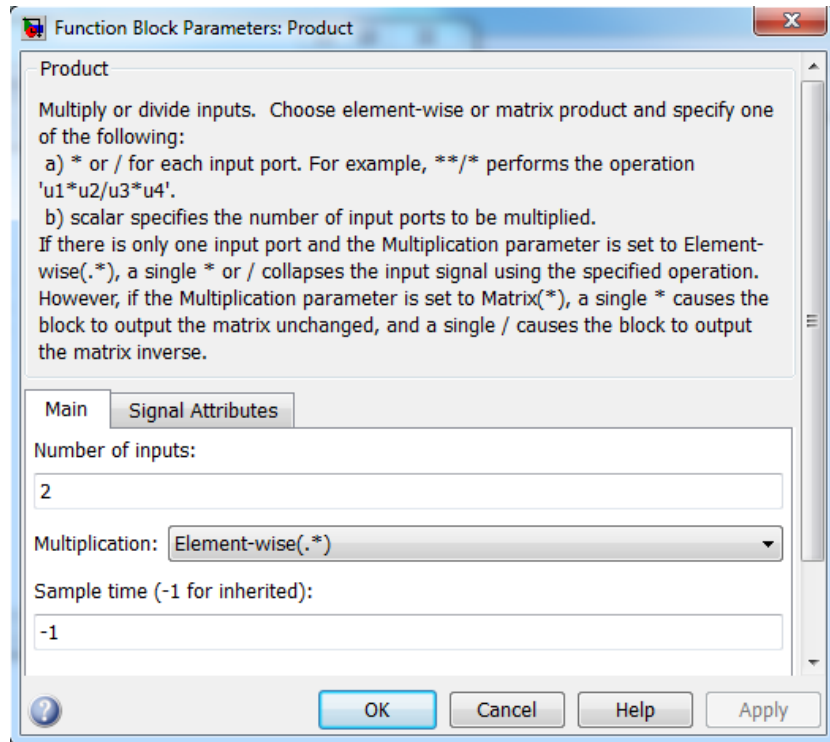


Figure 2.16: Dialog box of Product

Parameters of Product block:

Number of inputs: It specifies the number of inputs. By default its value is set to 2.

Multiplication: Specifies the type of multiplication i.e. whether *element-wise* (.*) or *matrix* (*).

When the value of the **Multiplication** parameter is Element-wise(*), the Product block is in *Element-wise mode*, in which it operates on the individual numeric elements of any nonscalar inputs.

When the value of the **Multiplication** parameter is Matrix(*), the Product block is in *Matrix mode*, in which it processes nonscalar inputs as matrices.

2.4.3.7 Sqrt

For the access of Sqrt block in Simulink, it should be proceeded with following flow:

Simulink -> Blocks -> Math Operations -> Sqrt, Signed Sqrt, Reciprocal Sqrt.

Calculates the square root of the input.



Figure 2.17: Sqrt Block

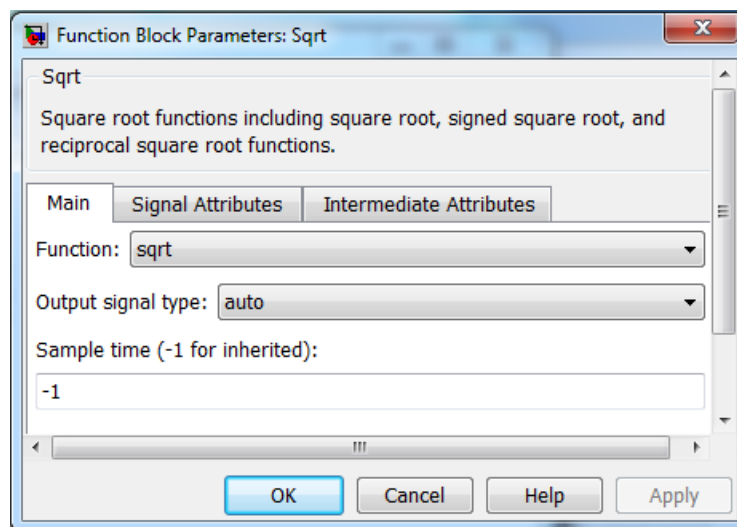


Figure 2.18: Dialog box of Sqrt

Parameters of Sqrt block:

Function: Specify the mathematical function. The block icon changes to match the function that is selected. Functions that can be selected from this parameter are *Sqrt*, *SignedSqrt*, *rSqrt*.

Output signal type: Specify the output signal type of the block as *auto*, *real*, or *complex*.

Sample time (-1 for inherited): Specify the time interval between samples. To inherit the sample time, this parameter is set to -1.

2.4.3.8 Constant

For the access of Constant block in Simulink, it should be proceeded with following flow:
Simulink -> Blocks -> Commonly Used -> Constant.



Figure 2.19: Constant Block

The Constant block generates a real or complex constant value.

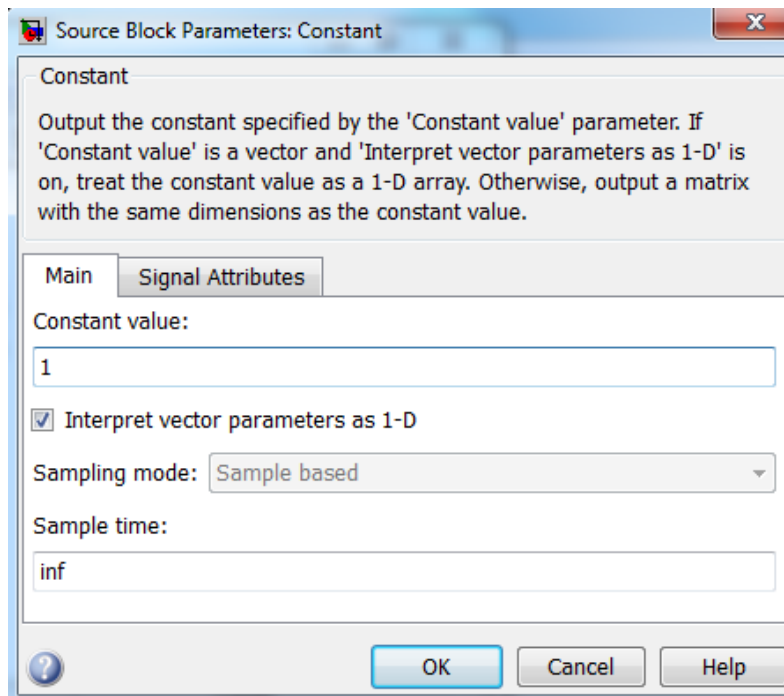


Figure 2.20: Dialog box of Constant

Parameters of Constant block:

Constant value: Constant block generates scalar, vector, or matrix output, depending on the dimensionality of this parameter and the setting of the **Interpret vector parameters as 1-D** parameter.

Interpret vector parameters as 1-D: If this box is checked, then the output is a one-dimensional signal. Otherwise, Constant block will treat Constant value parameter as a matrix.

Sampling mode: This parameter is active only if box of **Interpret vector parameters as 1-D** is unchecked. **Sampling mode** can be either *Sample based* or *Frame based*.

Sample time: Specify the interval between times that the Constant block output can change during simulation.

2.5 Summary

In this chapter implementation of MUSIC and ESPRIT algorithms were discussed in detail. Flowchart of these algorithms were also analyzed one by one. Each function and functional block implemented in MATLAB and Simulink were also mentioned and described.

Hence in this chapter, detail of all the simulation tools and the procedures used for study of MUSIC and ESPRIT algorithms were given.

CHAPTER III

RESULTS AND ANALYSIS

This chapter discuss on the experimental findings and comparison of the results of MUSIC with results of ESPRIT. For the experimentation of better resolution of angles, different parameters such as, number of array elements, number of users and space distribution between them, numbers of signal samples, Signal to Noise Ratio (SNR), processing time of these algorithms were taken as consideration.

These experiments considering above mentioned parameters were conducted with matlab and simulink.

3.1 Results from MATLAB

3.1.1 Error from MUSIC and ESPRIT with varying angle difference of signals

Fig. 3.1 and 3.2 give the plot of error from MUSIC and ESPRIT algorithms in percentile with respect to varying angle difference between two signals. For this plot two signals and four antenna elements were considered for simulation. The number of samples taken for this simulation was 1000 and SNR ratio was 10dB. Fig. 3.1 gives the plot for angle difference of 1 upto 100 while fig. 3.2 gives the plot for angle difference from 1 upto 10.

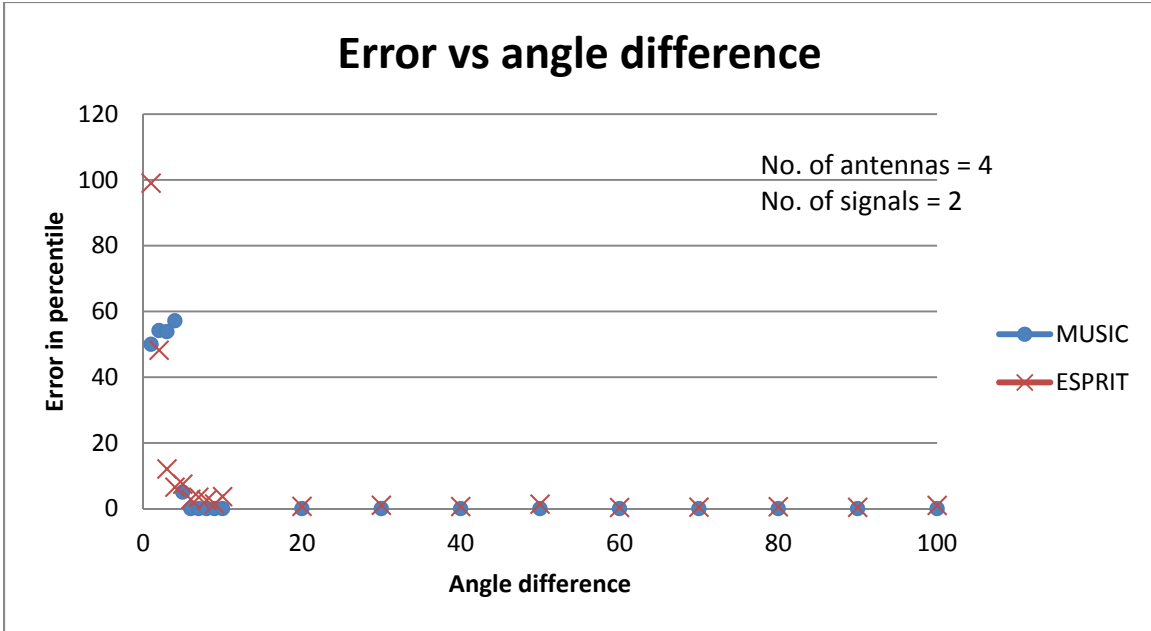


Figure 3.1: Errors from MUSIC and ESPRIT algorithms vs angle difference between two input signals when number of antenna elements is 4

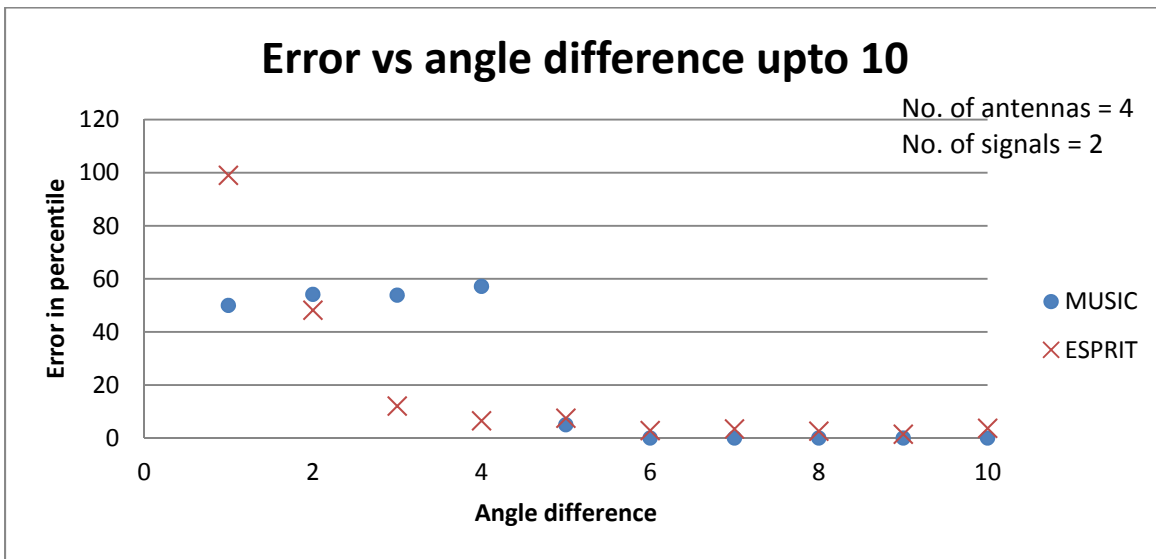


Figure 3.2: Errors from MUSIC and ESPRIT algorithms vs angle difference upto 10 between two input signals when number of antenna elements is 4

From fig. 3.2 it can be seen that, when difference of angle is below 2 degrees, error for MUSIC algorithm is less than ESPRIT. As angle difference increases error from ESPRIT decreases

rapidly than that of MUSIC. For this set up when angle difference between two signals reached 6 degrees, MUSIC gave 100% accurate result.

With consistent 0% error from MUSIC beyond 6 degrees of difference between two incoming signals, it can be implied that accuracy of MUSIC is better than that of ESPRIT for different angle difference cases.

Fig. 3.3 and 3.4 give the plot of error in percentile for both of the algorithms with respect to angle difference when number of antenna elements was taken as 7. Rest of the parameters were considered as same as that for fig. 3.1 and 3.2. Fig. 3.3 gives the error for both of the algorithms with respect to angle difference till 100 while fig. 3.4 gives the same plot upto angle difference of 10 between two signals.

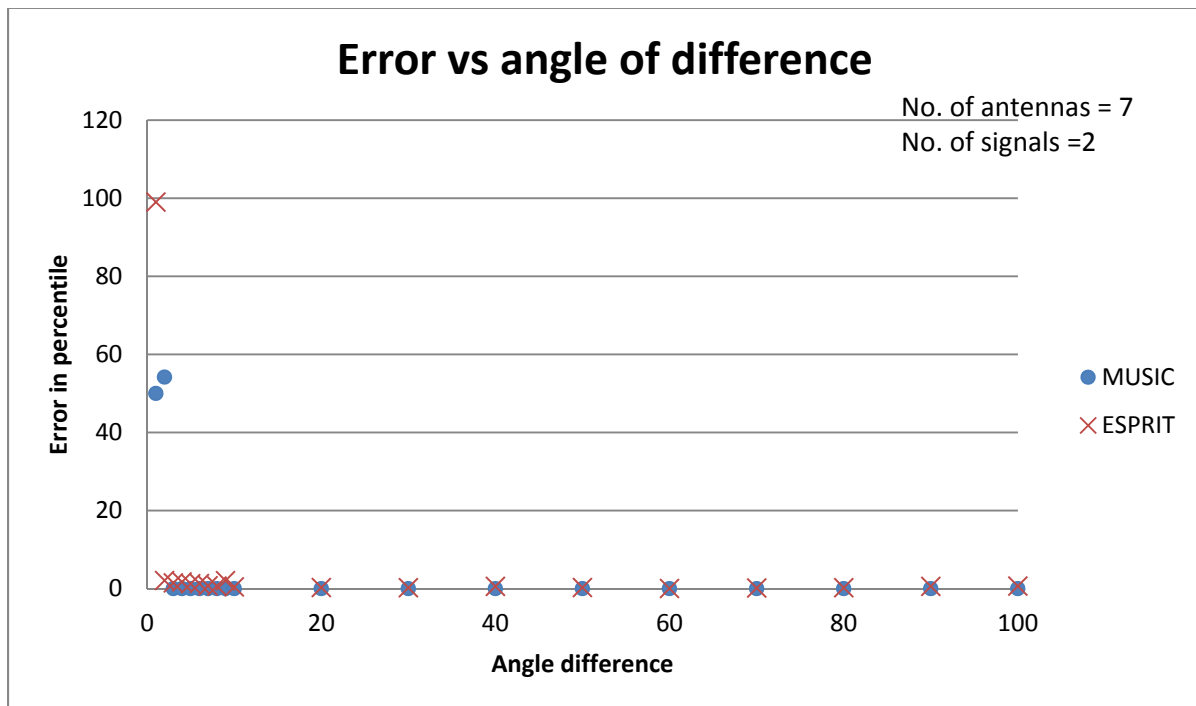


Figure 3.3: Errors vs angle difference between two input signals when number of antenna elements is 7

From fig. 3.4 it can be seen that MUSIC algorithms gives 0% error when the angle difference between two signals is increased to 3. Comparing the plots from fig. 3.2 and 3.4 it can be implied that, for the same angle difference, as the number of antenna elements increases, accuracy in angle estimation also increases.

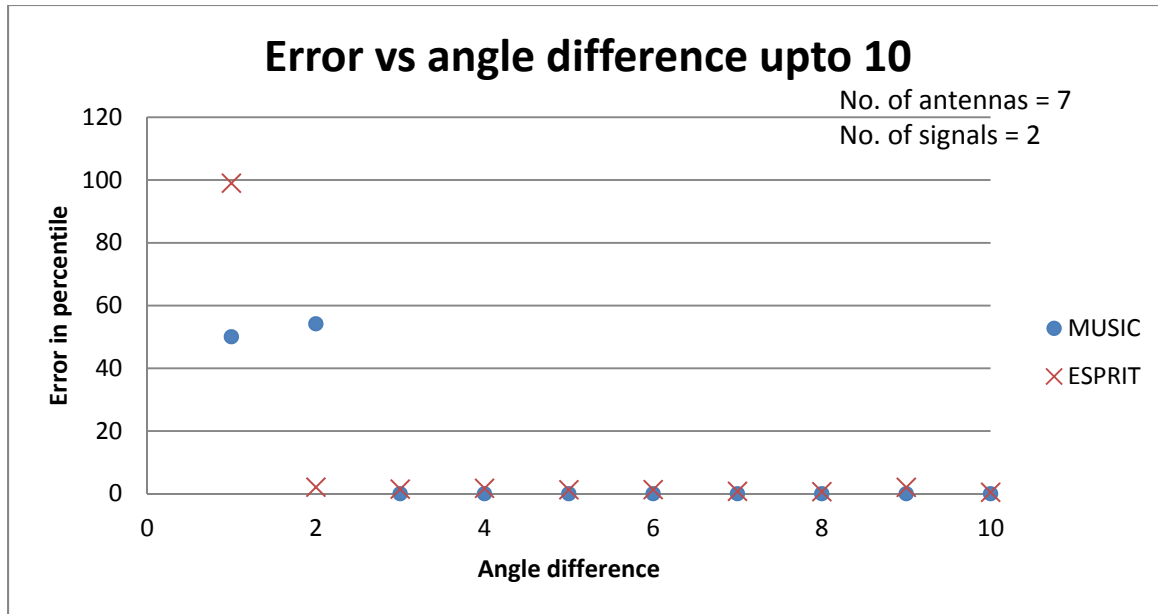


Figure 3.4: Error vs angle difference upto 10 between two input signals when number of antenna elements is 7

3.1.2 Error Vs. number of antenna elements

Fig. 3.5 gives plot of error in angle estimation from MUSIC and ESPRIT algorithms for different number of antenna elements. For plot in fig. 3.5, number of signals, SNR ratio and number of signal samples of signals were taken as 2, 10 dB and 1000 respectively. Keeping all other parameters constant and changing the number of antenna elements, from fig. 3.5 it can be observed that the error from both MUSIC and ESPRIT decreases with the increase in number of antenna elements. Also, it can be observed that error in angle estimation from MUSIC is much less than that of error in angle estimation from ESPRIT algorithm. This implies that the accuracy

from MUSIC algorithm is much higher than that of ESPRIT algorithm, and it can also be concluded that MUSIC has high resolution than that of ESPRIT.

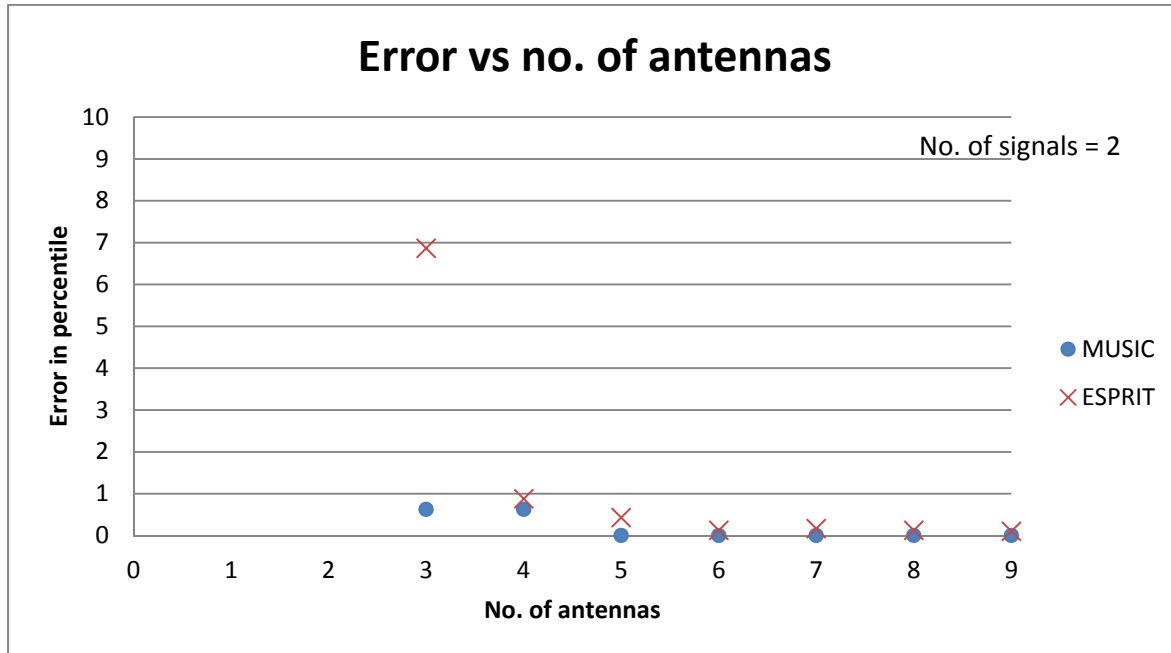


Figure 3.5: Errors from MUSIC and ESPRIT algorithm for different number of antenna elements with two input signals

3.1.3 Error Vs. number of samples of signals

Fig. 3.6 and 3.7 give the plot for error from MUSIC and ESPRIT with respect to different number of samples of signals. For these plots the number of antenna elements was taken as 4, no. of signals as two and SNR as 10 dB. From fig. 3.6 and 3.7 it can be observed that the error in angle estimation is very high and fluctuating below 100 numbers of samples of a signal. Error gradually decreases with increase in samples numbers. Above 100 samples too, the error rate is not satisfactory till the sample number reaches 500. Beyond 500 numbers of samples, the accuracy from both of the algorithms is very good though the accuracy of MUSIC was found better than that of ESPRIT. Hence from this plot it can be concluded that the number of samples

of signals should be always greater than 500 for better accuracy. It can also be concluded that the resolution of MUSIC is better than that of ESPRIT.

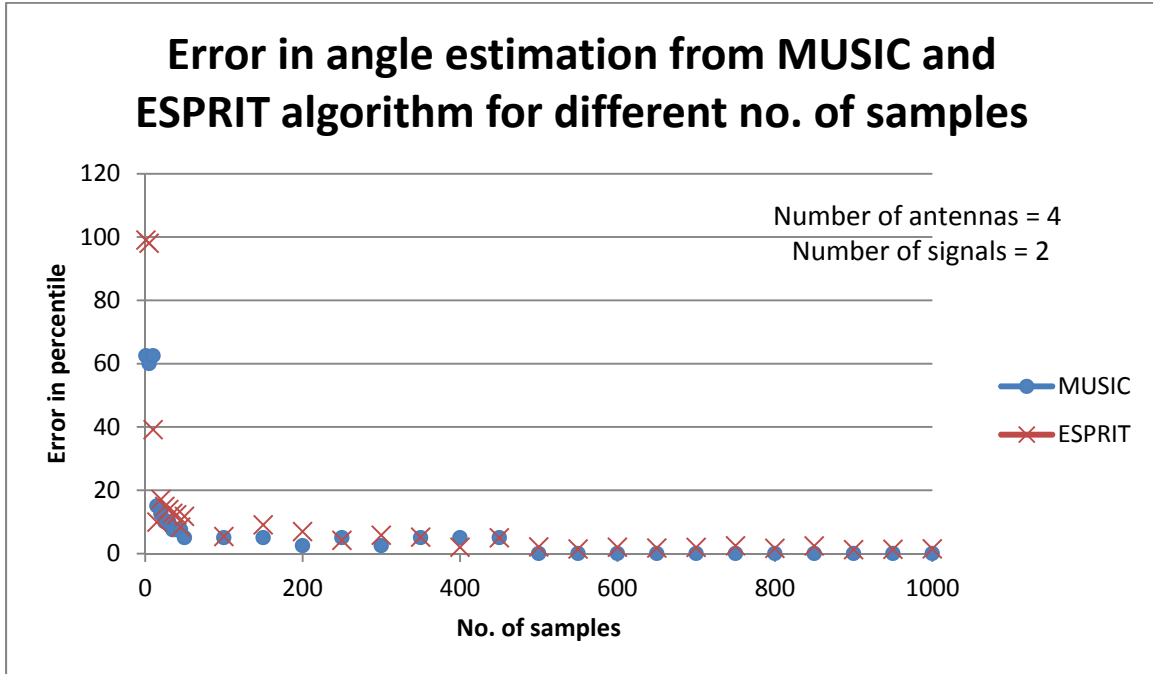


Figure 3.6: Error in angle estimation from MUSIC and ESPRIT algorithm for different number of sample of signals

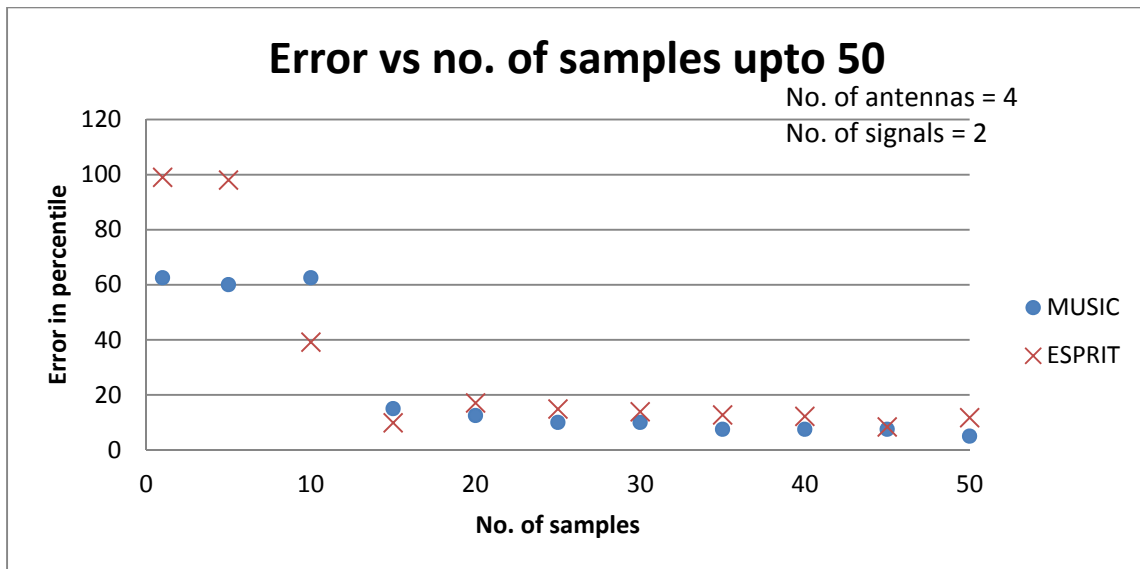


Figure 3.7: Error in angle estimation from MUSIC and ESPRIT algorithm for different number of samples of signals upto 50

3.1.4 Ratio of MUSIC processing time to ESPRIT processing time with respect to number of arriving signals

Plot of fig. 3.8 gives the ratio of MUSIC processing time to ESPRIT processing time with respect to different number of arriving signals. To obtain the data of fig. 3.10, the number of antenna elements was taken as 8. From fig. 3.8, we can observe that the ratio of MUSIC processing time to ESPRIT processing time is almost constant for different number of arriving signals. From this it can be concluded that the ratio of MUSIC to ESPRIT processing time will be almost constant for any number of incoming signals.

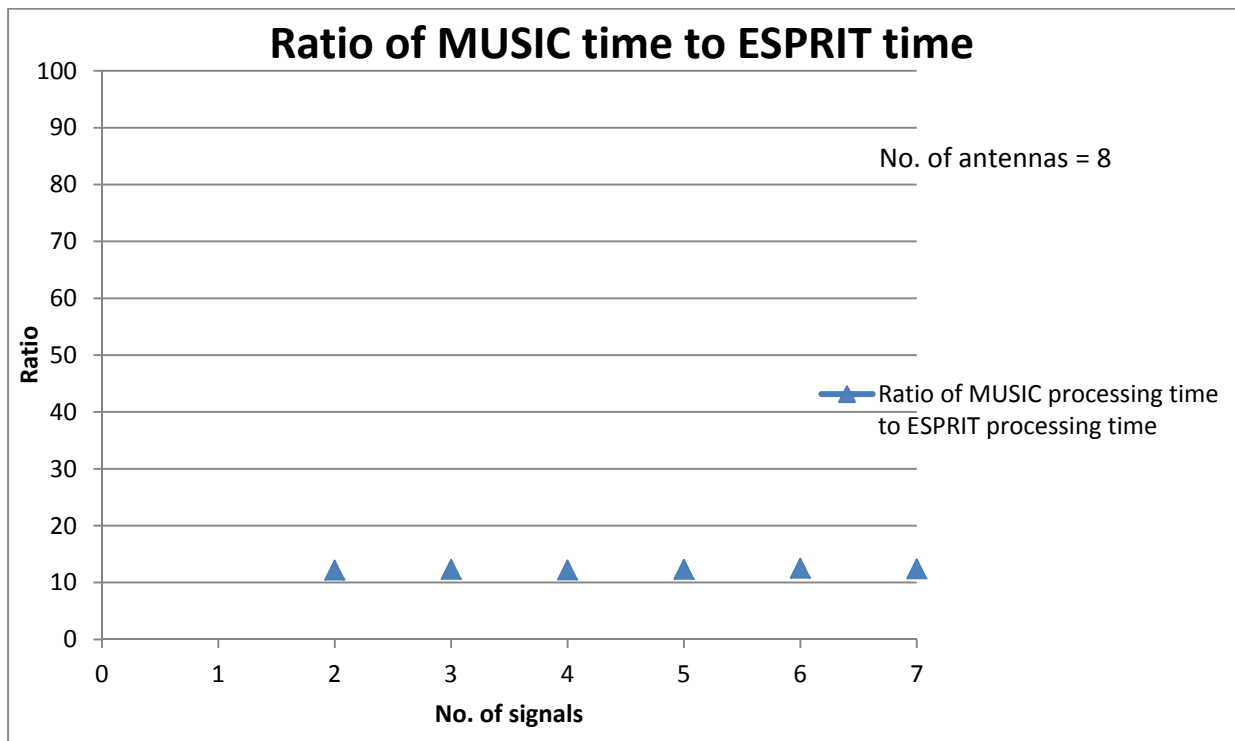


Figure 3.8: Ratio of MUSIC processing time to ESPRIT processing time vs number of signals

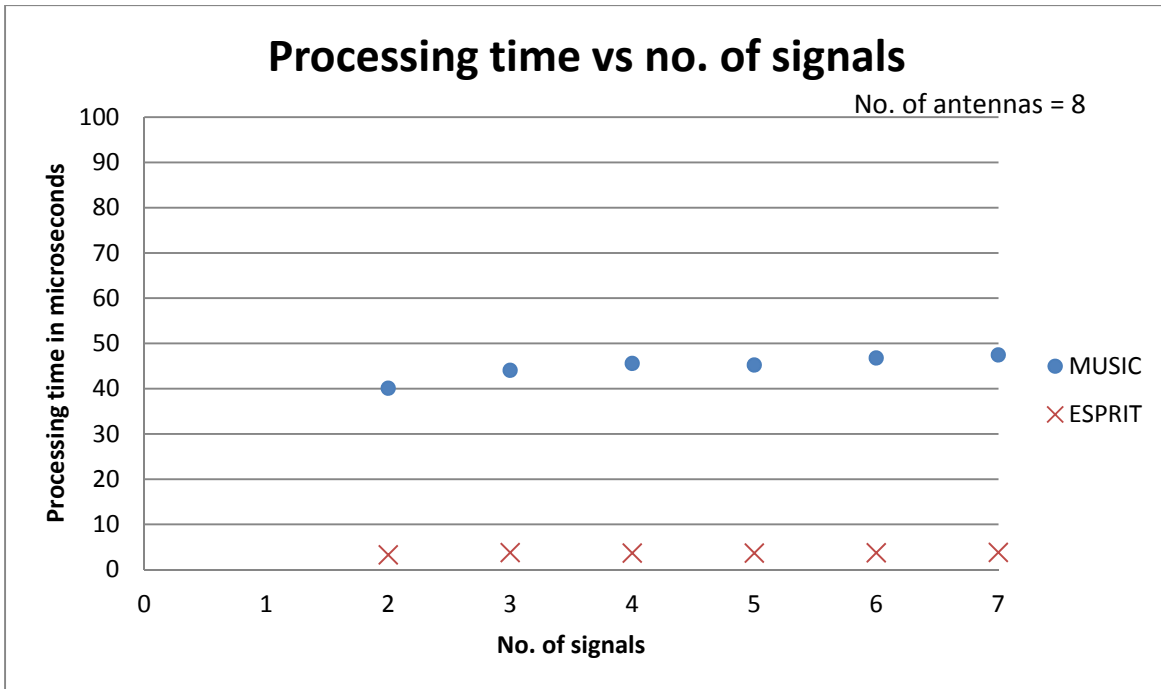


Figure 3.9: Processing time of MUSIC and ESPRIT in microseconds vs number of signals

Fig. 3.9 gives the plot of processing time of MUSIC and ESPRIT in terms of microseconds. From this plot it can be seen that the processing time of MUSIC is much higher than that of ESPRIT. MUSIC processing time is between 10 to 15 times of ESPRIT processing time. It can also be observed from fig. 3.9 that the processing time of MUSIC as well as ESPRIT is slightly increasing with the increase in number of incoming signals. From this it can also be implied that processing time for these algorithms increases with increase in number of incoming signals.

3.1.5 Error vs. number of signals

Fig. 3.10 shows the plot of error from MUSIC and ESPRIT with respect to number of signals. To obtain this plot the number of signals, number of antennas, number of signal samples and SNR ratio were taken as 2, 8, 1000 and 10dB respectively. From this plot it can be seen that with the increase in number of signals, error in angle estimation also increases from both of the algorithms.

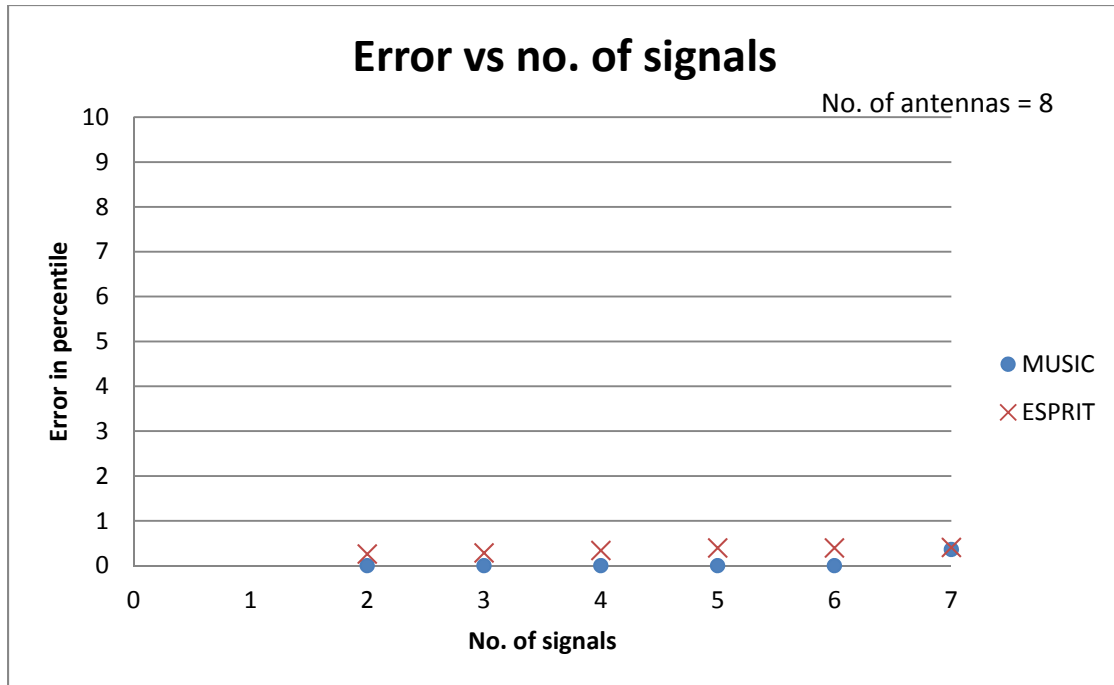


Figure 3.10: Error from MUSIC and ESPRIT with respect to number of signals

In this plot, error from ESPRIT is gradually increasing with increase in number of signals from 2 to 7. While for MUSIC, error in angle estimation was 0% till the number of signals was 6, and then the error increased for MUSIC when number of signals reached 7. From this result it can be concluded that error in angle estimation increases with the number of signals, and also the error in ESPRIT was more than that of MUSIC with the change in incoming number of signals.

3.1.6 Error with respect to SNR

Fig. 3.11 shows the plot of error in angle estimation from MUSIC and ESPRIT with respect to SNR ratio. For this plot number of antennas, number of signals and number of samples of signals for the simulation were taken as 4, 2 and 1000 respectively. From this plot it can be seen that increasing the SNR ratio has also increased the accuracy in angle estimation with decrease in error.

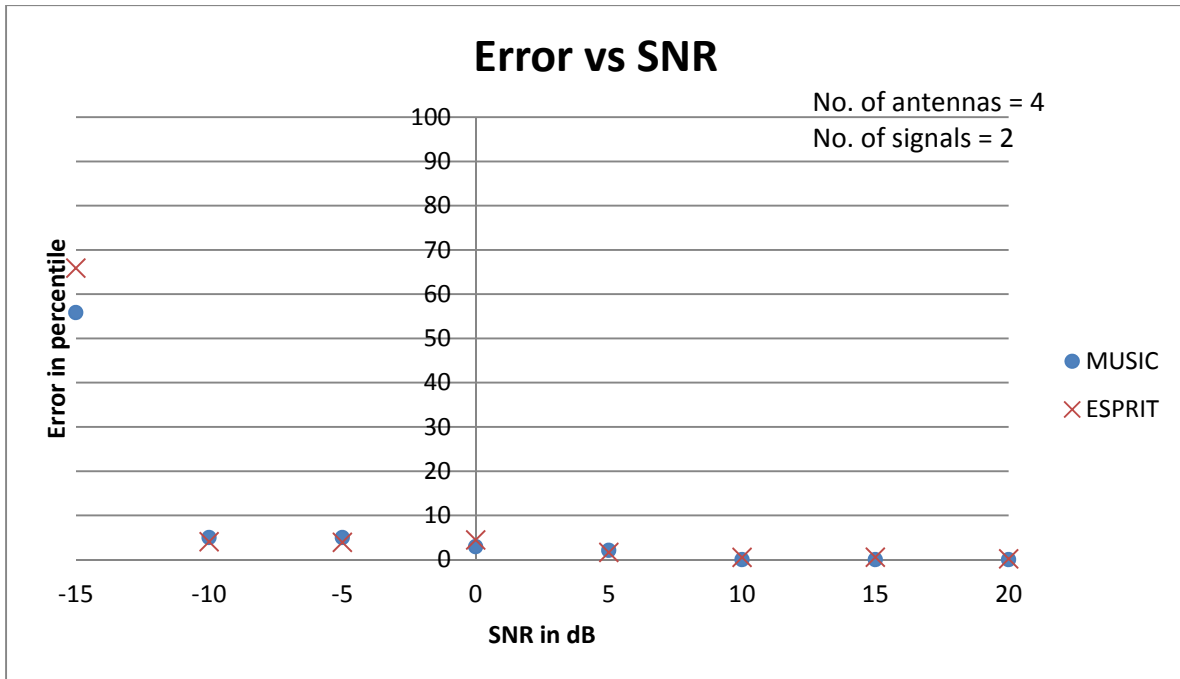


Figure 3.11: Error from MUSIC and ESPRIT with respect to number of arriving signals

In fig. 3.11 the error rate from both algorithms are very high when the value of SNR is -15dB. With the increase in SNR, error gradually decreases and error in angle estimation is almost 0% when the SNR is 5 dB. From this plot it implies that as SNR increases the accuracy of angle estimation also increases as well as it gives 100% accurate result for both MUSIC and ESPRIT above 5 dB.

3.2 Results from Simulink

Experiments that were done with the MATLAB were redone with Simulink too. While performing experiments with Simulink, some real time conditions were taken into consideration and then compared with the results from MATLAB simulations. For simulation in Simulink, inputs for angles were done in the basis of sectorization concept.

It was considered that each antenna elements in array has a range of its coverage area in terms of degree. Therefore, if a signal is received by a particular antenna element, the angle to be estimated for the simulation should be in between the range of coverage of particular antenna element. With this consideration all of the simulations performed with MATLAB were redone with Simulink and then results were compared.

3.2.1 Error vs angle difference

Fig. 3.12 shows the plot of error from MUSIC and ESPRIT with respect to angle difference between two signals with Simulink. For this plot the number of antenna elements, number of signals, number of samples of signals and SNR were taken as 4, 2, 1000 and 10 dB respectively.

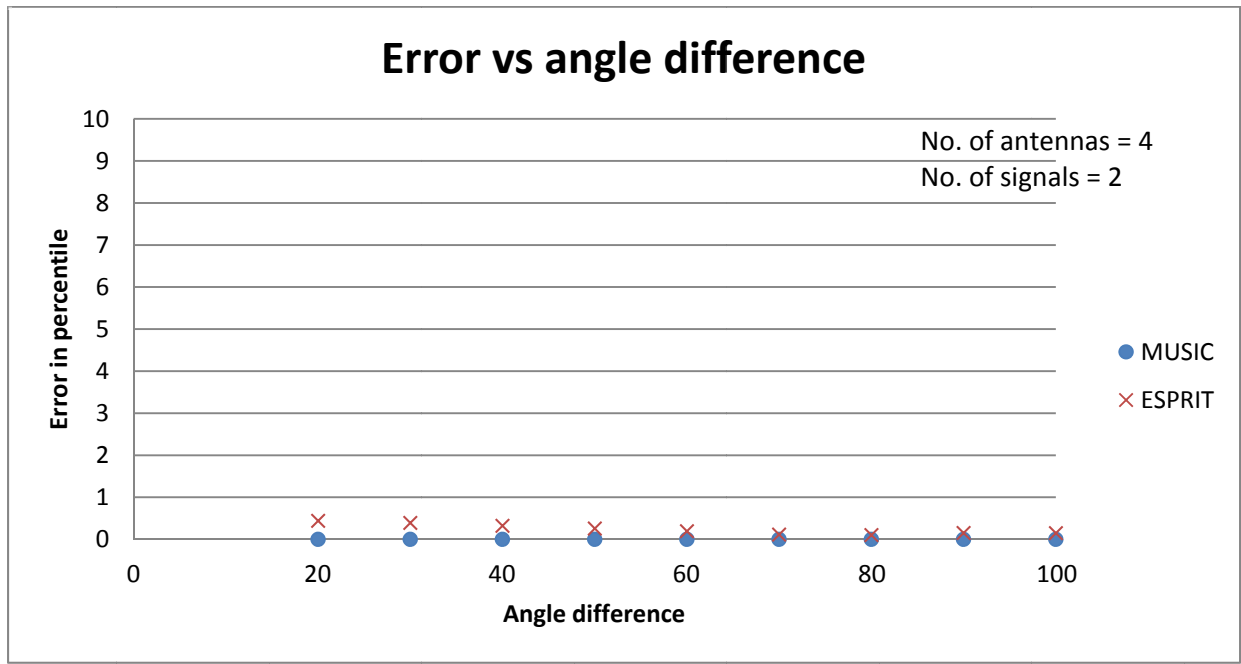


Figure 3.12: Error with respect to angle difference when number of antenna elements is 4 (with Simulink)

From this plot it can be seen that as the angle difference increases error in angle estimation from algorithms also decreases. In fig. 3.12 error from MUSIC is 0% from angle difference of 20

degree only. While for ESPRIT, error gradually decreases with the increase in angle difference and it reaches approximately 0% at angle difference of 40.

Fig. 3.13 shows the error plot with respect to angle difference taking all other parameters same besides the number of antenna elements different than that of fig. 3.12. For plot of fig. 3.13, the number of antenna elements was taken as 7. Comparing fig. 3.12 with fig. 3.13 it can be seen that, with increase in number of antenna elements error in angle estimation has also decreased. This is the exactly same result that we got from MATLAB simulation.

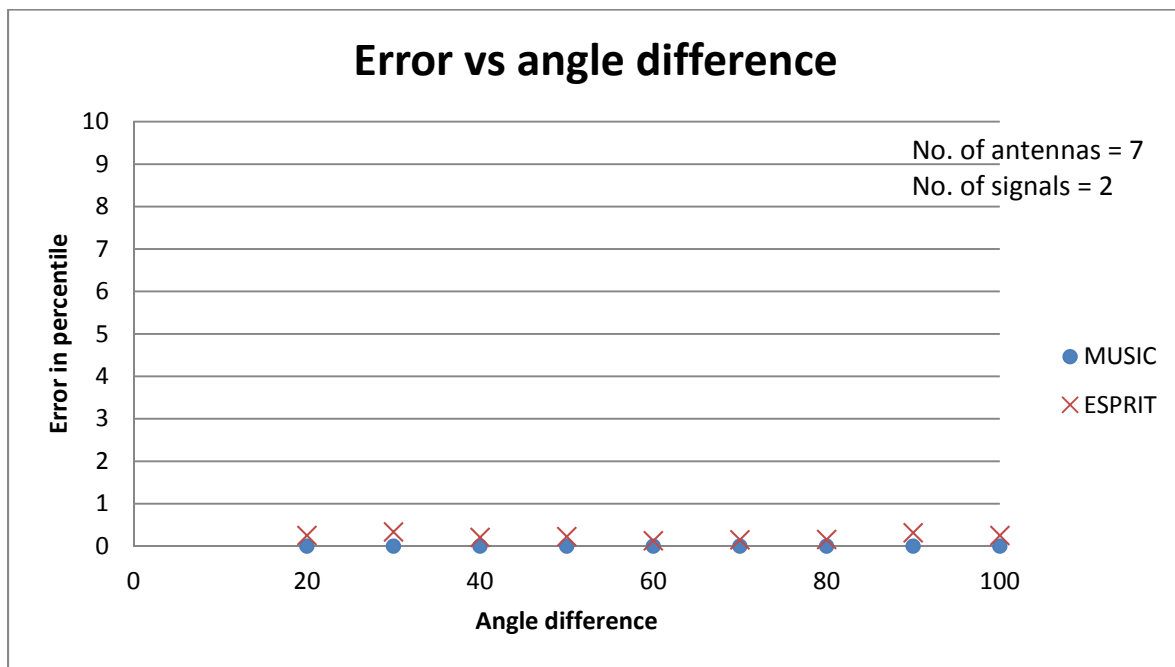


Figure 3.13: Error from MUSIC and ESPRIT with respect to angle difference when number of antenna elements is 7 (with Simulink)

Hence, comparing plot of fig. 3.1 with fig. 3.12 and fig. 3.3 with fig. 3.13 it can be said that these plots are almost exactly same. Similar result was obtained from Simulink as was from MATLAB for error plot with respect to angle difference.

From both of the results it can be concluded that MUSIC is less error prone compared to ESPRIT for different angle difference between two signals.

3.2.2 Error vs number of antenna elements

Fig. 3.14 shows the plot of error in percentile from MUSIC and ESPRIT algorithm for different number of antenna elements with Simulink. To obtain this plot, parameter values were taken as follows; number of signals, number of signal samples and SNR as 2, 100 and 10 dB respectively.

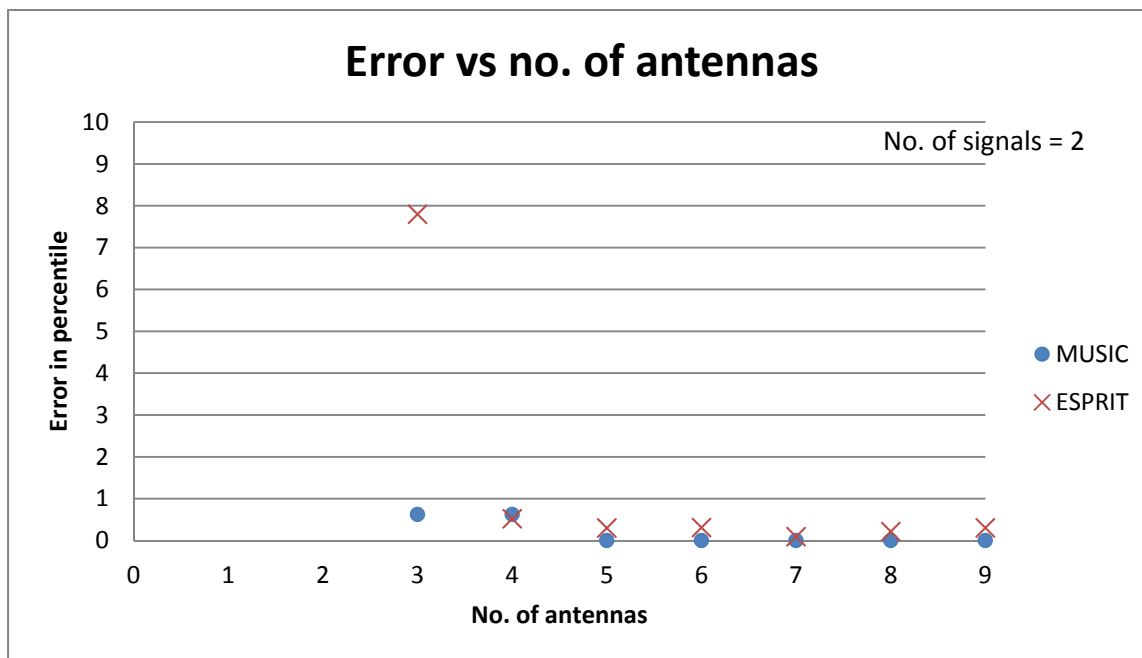


Figure 3.14: Error from MUSIC and ESPRIT with respect to number of antenna elements (with Simulink)

From fig. 3.14 it can be observed that, as the number of antenna elements increases error in angle estimation decreases. Here error from MUSIC algorithm is less than that from ESPRIT.

Comparing fig. 3.5 from MATLAB with fig. 3.14 from Simulink, we can conclude that both of them gives the same result, i.e. error from both of the algorithms decreases with the increase in number of antenna elements, and also error from MUSIC is less than that from ESPRIT.

3.2.3 Error vs number of samples

Fig. 3.15 and 3.16 are plots of error in percentile from MUSIC and ESPRIT with respect to different sample numbers. For these plots the number of antenna elements, number of signals and SNR were taken as 4, 2 and 10 dB respectively.

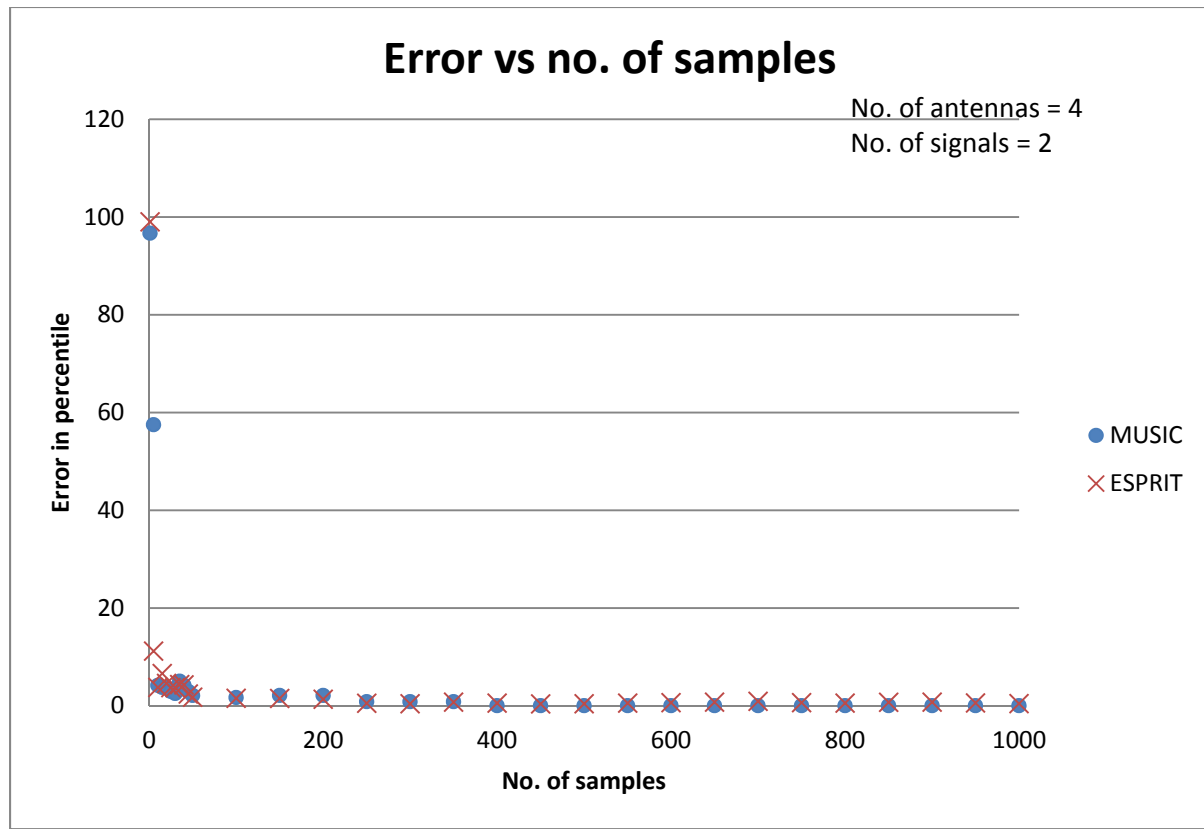


Figure 3.15: Error from MUSIC and ESPRIT algorithms for different number of samples (with Simulink)

Plot in fig. 3.15 and 3.16 show that the error from both of the algorithms decreases with increase in number of samples. From these plots it can be seen that the error rate from both of these algorithms are very high below 10 numbers of samples. Above 200 samples it can be seen that the error from these algorithms are approximately 0%.

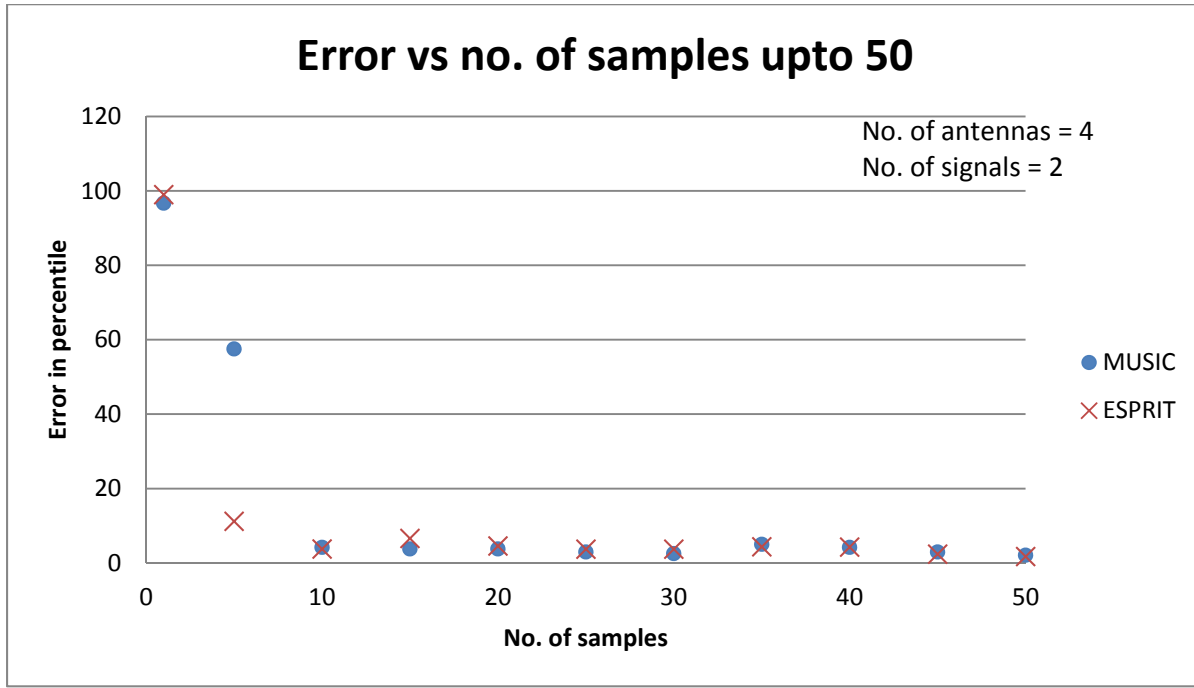


Figure 3.16: Error from MUSIC and ESPRIT algorithms for with respect to number of samples upto 50 (with Simulink)

Comparing plots of fig. 3.6 from MATLAB and fig. 3.15 from Simulink it can be said that they are approximately similar. In both of these plots error from both of the algorithms are very high with sample number below 50 and with increase in sample number, error decreases gradually and it is approximately 0% above 500. It can also be observed that almost for any number of samples, error from MUSIC is slightly less than that from ESPRIT.

3.2.4 Processing time and ratio of MUSIC processing time to ESPRIT processing time with Simulink

To obtain the plot for processing time of MUSIC and ESPRIT, simulation was done with Simulink considering number of antenna elements as 8, number of samples as 1000 and SNR as 10 dB. Keeping these parameters constant and changing number of signals to observe the

response for processing time from both of these algorithms, plot of fig. 3.17 was obtained as the result of simulation.

From the plot of fig. 3.17 it can be seen that with the increase in the number of incoming signals, processing time for angle estimation of the algorithms also increases. Though this time difference is not very large, still it can be concluded that with the increase in number of signals, processing time for these algorithms also increases.

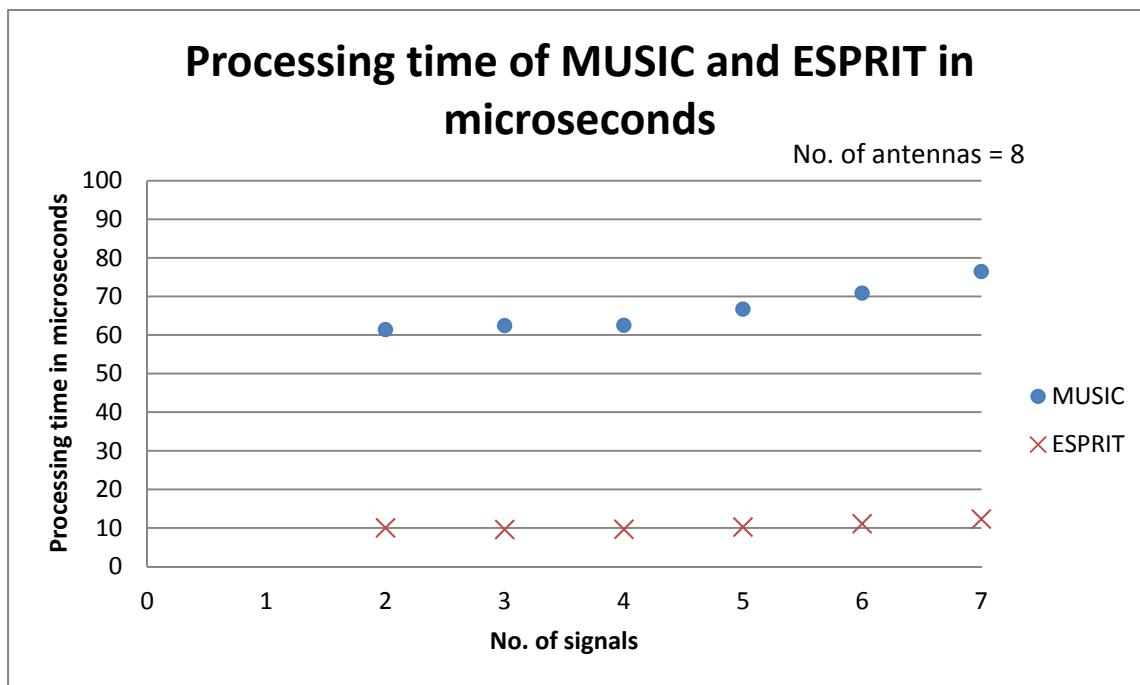


Figure 3.17: Processing time of MUSIC and ESPRIT for angle estimation (with Simulink)

The plot shown in fig. 3.18 gives the ratio of processing time for MUSIC to ratio of processing time for ESPRIT algorithm for different number of incoming signals. From this plot it can be seen that the ratio of MUSIC to ESPRIT is almost constant for any number of arriving signals.

Hence from plots of fig. 3.17 and 3.18 it can be implied that the rate of change in processing time from both of these algorithms is almost same as the ratio between processing time for these algorithms is almost constant.

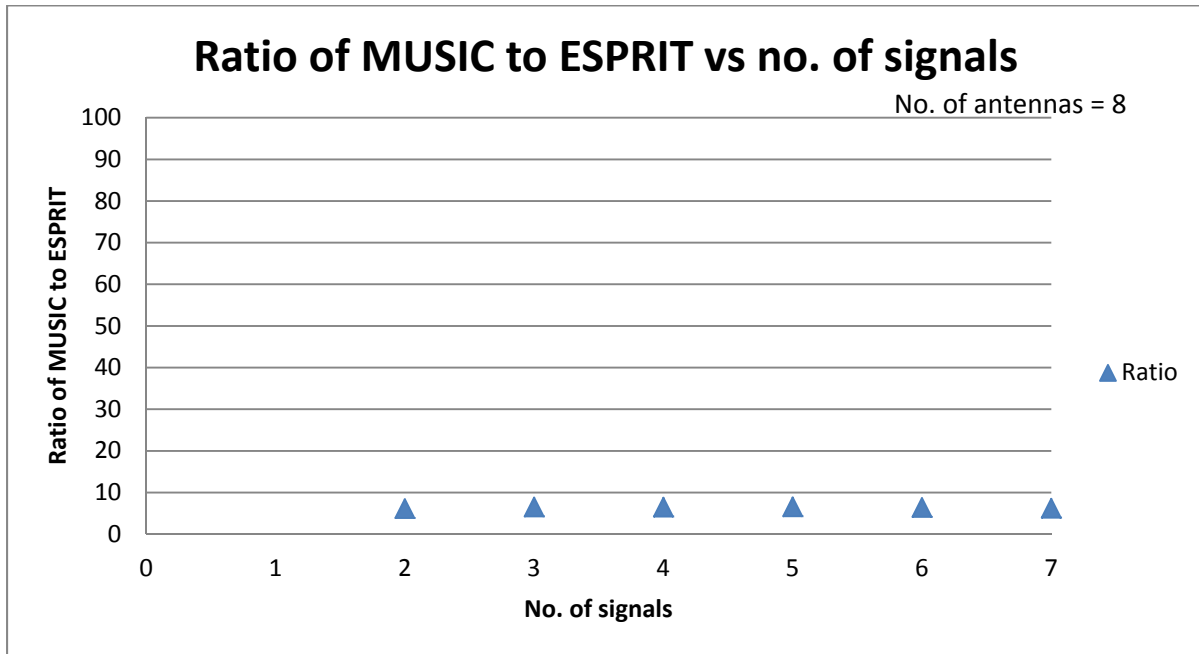


Figure 3.18: Ratio of processing time for MUSIC to ESPRIT with respect to number of incoming signals (with Simulink)

Comparing plot from fig. 3.9 and 3.17 it can be observed that the processing time for both MUSIC and ESPRIT is more for Simulink than that for MATLAB. The reason for simulink to take longer processing time must be the use of source blocks and other functional blocks used along with the matlab functional block. Use of these blocks in Simulink increases the interfacing time between the blocks. So, that is the reason for longer processing time for these algorithms with Simulink than that with MATLAB.

Also from fig. 3.8 and 3.18 it can be observed that the ratio of processing time for MUSIC to processing time for ESPRIT has decreased for Simulink than that of MATLAB. The reason for decrease in ratio for Simulink is the increase in processing time for angle estimation from

Simulink. With increase in processing time for the reason mentioned above, the proportion for increment in the processing time differs for these two algorithms and as the result there was overall change in the ratio of processing time of these algorithms.

Hence comparing the plots for processing time and ratio of processing time from MATLAB and Simulink, it can be concluded that, though the processing time and ratio of MUSIC's processing time to ESPRIT's processing time from Simulink increased and decreased respectively compared to that with MATLAB, the tendency of plot for both processing time and ratio of processing time is similar. For both MATLAB and Simulink processing time slightly increased with increasing number of incoming signals. Also, the ratio of processing time of MUSIC to ESPRIT is almost constant for both MUSIC and ESPRIT.

3.2.5 Error with different number of incoming signals

Plot of error from MUSIC and ESPRIT for different number of incoming signals is shown in fig. 3.19. To obtain this plot, parameters like number of antenna elements, number of signal samples and SNR were taken as 8, 1000 and 10 dB respectively.

From the plot of fig. 3.19 we can observe that, error from MUSIC and ESPRIT increases with the increase in number of incoming signals. For 8 number of antenna elements we can see that error from these algorithms is approximately 0% till the number of signals reaches 6, but when the number of incoming signals reaches 7, we can see that the error from both of these algorithms increases.

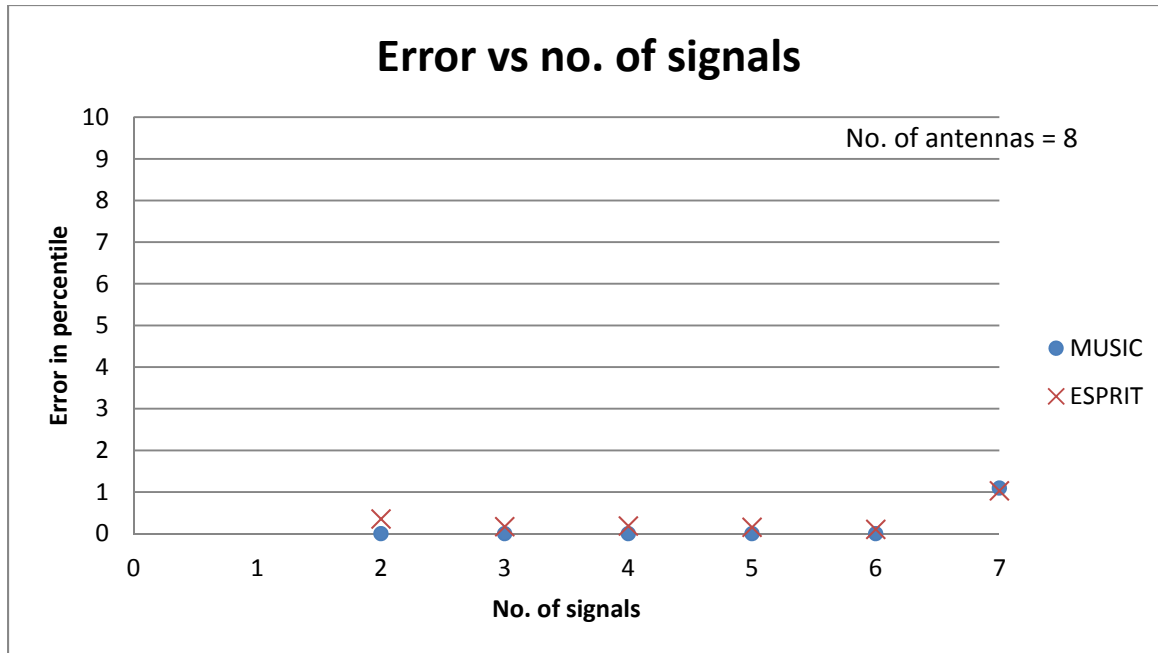


Figure 3.19: Error with respect to number of incoming signals (with Simulink)

Comparing fig. 3.10 from MATLAB and fig. 3.19 from Simulink for error in angle estimation with respect to number of incoming signals, it can be concluded that, results from both MATLAB as well as Simulink are similar i.e. pattern of plot in both of these plots are similar and both of these plot indicates that error from both of these algorithms increases with increase in number of incoming signals after number of incoming signals reaches certain value.

3.2.6 Error with SNR ratio

Plot from fig. 3.20 is of the error from MUSIC and ESPRIT for different values of SNR. For this plot values of parameters were considered as follows; number of antenna elements as 4, number of incoming signals as 2 and number of samples of signals 1000.

From fig. 3.20 it can be analyzed that, though the error from MUSIC is comparatively lower than that of ESPRIT, error from both of the algorithms is very high for the negative value of SNR ratio. Error settles down to 0% as the value of SNR ratio tends to positive value from negative

value. Error from MUSIC settles down to 0% faster than that of ESPRIT as the value of SNR increases.

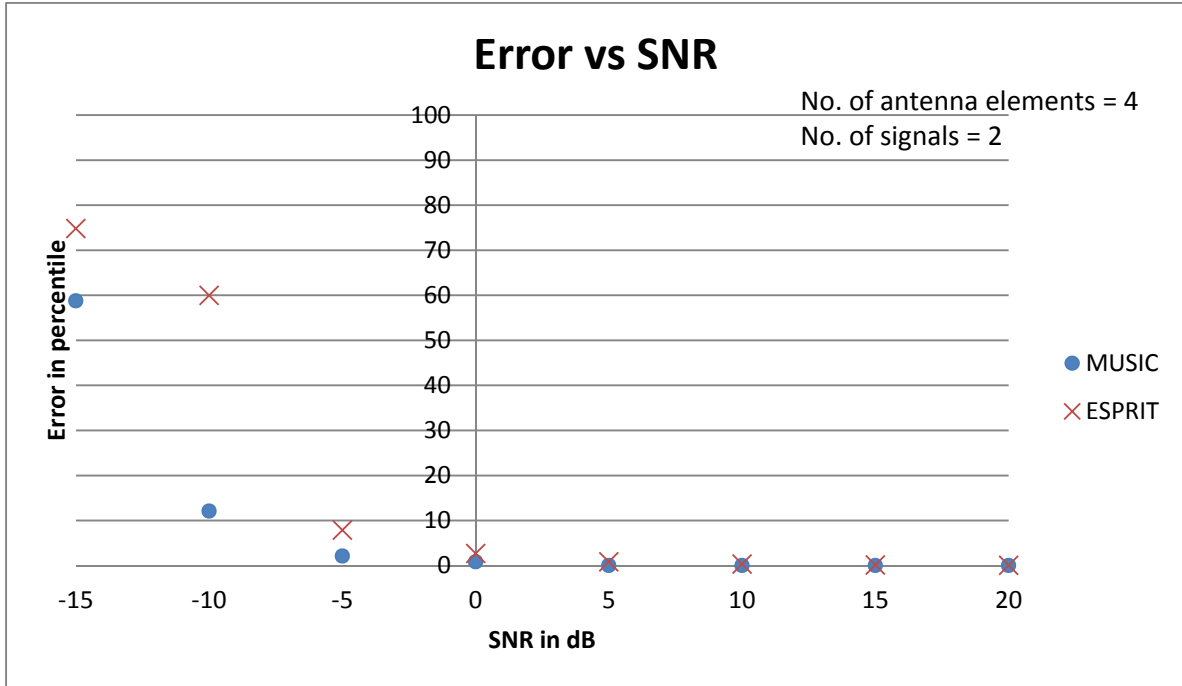


Figure 3.20: Error with respect to SNR ratio (with Simulink)

Comparing fig. 3.11 from MATLAB with fig. 3.20 from Simulink for error in angle estimation from MUSIC and ESPRIT with change in SNR values, we can conclude that both of the plots give same result. Their output pattern is similar in these plots. From these results it can be concluded that, with the increase in SNR ratio accuracy in angle estimation from MUSIC and ESPRIT also increases, and also MUSIC have higher accuracy rate than that of ESPRIT in angle estimation with change in SNR ratio.

3.3 Analysis

After observance and analysis done from above mentioned simulation from both Simulink and MATLAB it can be concluded that Simulink and MATLAB gave almost same results and the

pattern of plots from both were similar for almost all of the cases. Though the pattern of results were same, there was difference in Simulink and MATLAB results in the cases of processing speed and ratio of processing time of MUSIC to ESPRIT. This difference was due to the interfacing time required between different Simulink's blocks in Simulink. Hence, from all of the obtained results it can be concluded that beside the processing speed, all of the results from MATLAB and Simulink is same.

Also, from the results of all the simulation done with MATLAB and Simulink it can be concluded that MUSIC is less prone to error compared to ESPRIT for different cases of simulation, i.e. for varying difference in angles between two signals, varying number of antenna elements, different number of signals, different number of samples and different SNR ratio. Hence, from the analysis of all the results obtained from MATLAB and Simulink, for angle estimation from MUSIC and ESPRIT it can be concluded that MUSIC algorithm will be best for the implementation for estimation of arrival angle of incoming signals as it is more accurate than ESPRIT for almost all of the cases that has to be considered for the angle estimation.

CHAPTER IV

CONCLUSION AND RECOMMENDATIONS

4.1 Conclusion

The evolution of concept of cell to development of advance technology of smart antenna is discussed in this dissertation. Different DOA estimation and beamforming techniques are also mentioned in the sequence. Main objective of this thesis was to do performance analysis and then a comparison between MUSIC and ESPRIT algorithm. So these two algorithms were discussed in detail first, then the methodologies implemented for the performance analysis were described, and at last results from these algorithms were discussed.

From results obtained from MATLAB and Simulink, it was seen that Simulink and MATLAB gave almost same results and the pattern of plots from both were similar for almost all of the cases. Result from these two tools was found different only in the case of processing speed and ratio of processing time of MUSIC to ESPRIT. This difference was due to the interfacing time required between different Simulink's blocks used in Simulink. So, with all of the results obtained it can be concluded that beside the processing speed, all of the results from MATLAB and Simulink are same. Hence, performing experiments for MUSIC and ESPRIT algorithms will not get much affected with whether they are experimented with MATLAB or Simulink. Comparing results from MUSIC algorithm with that of ESPRIT algorithm it was found that,

MUSIC is less prone to error compared to ESPRIT for different cases of simulation, i.e. for varying difference in angles between two signals, varying number of antenna elements, different number of signals, different number of samples and different SNR ratio. Hence, from the analysis of all the results obtained from MATLAB and Simulink, for angle estimation from MUSIC and ESPRIT it can be concluded that MUSIC algorithm will be best for the implementation for estimation of arrival angle of incoming signals as it gives more accurate result than ESPRIT for almost all of the cases that needs to be considered for the angle estimation.

4.2 Recommendations

Though it is concluded from the analysis done from the results of experiments that MUSIC algorithm is better over ESPRIT, it has also should be taken into consideration that MUSIC is a computationally intensive algorithm. So, future work in the study of DOA algorithms should be in development of an algorithm which is not computationally intensive and have very good accuracy.

Also, as these experiments were done for an environment of stationary user and interferers, the future work will be to analyze all these experiments in dynamic scenario with improvement in SNR ratio.

REFERENCES

- 1) S. Bellofiore, C.A. Balanis, J. Foutz and A.S. Spanias, "Smart-Antenna Systems for Mobile Communication Networks Part 1: Overview and Antenna Design", *IEEE Antennas and Propagat. Mag.*, Vol 44, No. 3, pp. 145-154, June 2002.
- 2) M. Chryssomallis, "Smart Antennas", *IEEE Antennas and Propagat. Mag.*, Vol 42, No. 3, pp. 129-136, June 2000.
- 3) T.R. Rappaport, *Wireless Communications, Principles and Practice*, 2nd Edition, New Delhi, New York, Prentice Hall, 2008.
- 4) C.A. Balanis, *Antenna Theory, Analysis and Design*, 3rd Edition, New Jersey, John Wiley & Sons, 2005.
- 5) M.J. Ho, G.L. Stuber and M.D. Austin, "Performance of Switched-Beam Smart Antenna for Cellular Radio Systems", *IEEE Transaction on Vehicular Technology*, Vol. 47, No. 1, pp. 10-19, February 1998.
- 6) International Engineering Consortium, *Smart Antenna Systems*, an on-line tutorial found on http://www.iec.org/online/tutorials/smart_ant/index.html.
- 7) S. Sanayei and A. Nosratinia, "Antenna Selection in MIMO Systems", *IEEE Communications Mag.*, pp. 68-73, October 2004.
- 8) I. Stevanovic, A. Skrinverik and J.R. Mosig, *Smart Antenna Systems for Mobile Communications*, Ecole Polytechnique Federale de Lausanne, January 2003.

- 9) L. Zhou, D. Huang, H. Duan and Y. Chen, "A Modified ESPRIT Algorithm Based on A New SVD Method for Coherent Signals", Information and Automation (ICIA), IEEE International Conference, June 2011.
- 10) H. Jiang, G. Yang and G. Lu, "A Modified ESPRIT Algorithm for Signal DOA Estimation", Communication Technology and Application (ICCTA 2011), IET International Conference, Oct. 2011.
- 11) M. C. Roh, *A Base Station Smart Antenna System for CDMA Cellular*, S.B. Electrical Engineering and Computer Science, Massachusetts Institute of Technology, June 1998.
- 12) A. Gorokhov, D. A. Gore and A. J. Paulraj, "Receive Antenna Selection for MIMO Spatial Multiplexing: Theory and Algorithms", *IEEE transactions on signal processing*, Vol. 51, No. 11, November 2003.
- 13) F. E. Fakoukakis, S. G. Diamantis, A. P. Orfanides, and G. A. Kyriacou, "Development of an Adaptive and a Switched Beam Smart Antenna System for Wireless Communications", *Electromagnetics Waves and Applications*, Vol. 20, Issue 3, pp 399-408, 2006.
- 14) A. F. Molisch, M. Z. Win, Y. S. Choi and J. H. Winters, "Capacity of MIMO Systems with Antenna Selection", *IEEE transactions on wireless communications*, Vol. 4, No. 4, July 2005.
- 15) A. Dua, K. Medepalli and A. J. Paulraj, "Receive Antenna Selection in MIMO Systems using Convex Optimization", *IEEE transactions on wireless communications*, Vol. 5, No. 9, September 2006.
- 16) F. Gross, *Smart Antennas for Wireless Communications with MATLAB*, McGraw-Hill, 2005.

- 17) S. Bellofiore, C.A. Balanis, J. Foutz and A.S. Spanias, "Smart-Antenna Systems for Mobile Communication Networks Part 2: Beamforming and Network Throughput", *IEEE Antennas and Propagat. Mag.*, Vol. 44, No. 4, pp. 106-114, August 2002.
- 18) A. Kuchar, M. Tangemann and E. Bonek, "A Real-Time DOA-Based Smart Antenna Processor", *IEEE transactions on vehicular technology*, Vol. 51, No. 6, November 2002.
- 19) Q. Wu and D. R. Fuhrmann, "A Parametric Method for Determining the Number of Signals in Narrow-Band Direction Finding", *IEEE transactions on signal processing*, Vol. 39, No. 8, August 1991.
- 20) J. C. Liberti, Jr. and T. S. Rappaport, *Smart Antennas for Wireless Communications: IS-95 and Third Generation CDMA Applications*, Prentice Hall PTR, Upper Saddle River, NJ, 1999.
- 21) R.J. Weber and Y. Huang, "Hardware Analysis for Capon and MUSIC DOA estimation algorithms", *Antennas and Propagation Society International Symposium*, 2009, APSURSI '09, IEEE, pp 1-4, 1-5 June 2009.
- 22) H. Ke, Z. Xiaomin, H. Peng, Y. Yang and Y. Shi, "A DOA Estimation Algorithm without Source Number Estimation for Nonplanar Array with Arbitrary Geometry", *International Journal of Computer Theory and Engineering*, Vol. 2, No. 4, pp. 569-573, August, 2010.
- 23) A. K. Djedid and M. Fujita, "Adaptive Array Sensor Processing Applications for Mobile Telephone Communications", *IEEE transactions on vehicular technology*, Vol. 45, No. 3, August 1996.
- 24) A. Vesa, "Direction of Arrival Estimation using MUSIC and Root – MUSIC Algorithm", 18th Telecommunications forum TELFOR 2010, Serbia, Belgrade, pp 582-585, November 23-25, 2010.

- 25) T.N. Rao, V.S. Rao, "Implementation of MUSIC Algorithm for a Smart Antenna System for Mobile Communications", *International Journal of Scientific & Engineering Research*, Vol. 2, Issue 12, December-2011.
- 26) J. Axmon, M. Hansson and L. Sornmo, "A Signal Model Adapted ESPRIT Algorithm For Joint Estimation Of Spatial And Temporal Parameters In Vibrational Analysis Of Cylinders", 2002 IEEE Sensor Array and Multichannel signal processing workshop; SAM 2002, Rosslyn, VA, USA, 4-6 August, 2002.
- 27) L. C. Godara, "Application of Antenna Arrays to Mobile Communications, Part II: Beam-Forming and Direction-of-Arrival Considerations," *Proc. IEEE*, Vol. 85, No. 8, pp. 1195–1245, Aug. 1997.
- 28) R.S. Kawitkar, D.G. Wakde, "An approach for MUSIC algorithm in smart antenna system", IEEE International workshop on antenna technology, 2005, Singapore.
- 29) A. J. Weiss and M. Gavish, "Direction Finding Using ESPRIT with Interpolated Arrays", *IEEE transactions on signal processing*, Vol. 39, No. 6, pp 1473-1478, June 1991.
- 30) T.N. Rao, V.S. Rao, "Evaluation of MUSIC Algorithm for a Smart Antenna System for Mobile Communications", Devices, Circuits And Systems (ICDCS), 2012 International Conference, 15-16 March, pp. 67-71, 2012.
- 31) B. Ottersten and T. Kailath, "Direction-of-Arrival Estimation for Wide-Band Signals Using the ESPRIT Algorithm", *IEEE transactions on acoustics, speech, and signal processing*, Vol. 38, No. 2, pp 317-327, February 1990.
- 32) R. Roy, T. Kailath, "ESPRIT-Estimation of Signal Parameters via Rotational Invariance Techniques", *IEEE transactions on acoustics speech and signal processing*, Vol. 37. No. 7, July 1989.

- 33) M. H. E. Shafey, "ESPRIT Condition in Signal Parameter Estimation", Sarnoff Symposium, 2009, SARNOFF '09, IEEE, March 30 2009- April 1 2009.
- 34) S. Shahbazpanahi, S. Valaee and M. H. Bastani, "Distributed Source Localization Using ESPRIT Algorithm", *IEEE transactions on signal processing*, Vol. 49, No. 10, pp 2169-2178, October 2001.
- 35) C.R. Dongarsane, A.N. Jadhav, S.M. Hirikude, "Performance analysis of ESPRIT algorithm for smart antenna system", *International Journal of Communication Network and Security (IJCNS)*, Vol. 1, Issue 3, 2011.
- 36) V.C. Soon and Y.F. Huang, "An analysis of ESPRIT under random sensor uncertainties", *IEEE transactions on signal processing*, Vol. 40, No. 9, September 1992.
- 37) A. J. Weiss, B. Friedlander, "DOA and Steering Vector Estimation Using a Partially Calibrated Array", *IEEE transactions on aerospace and electronic systems*, Vol. 32, Issue 3, pp. 1047-1057, July 1996.
- 38) M. S. Amin, M. R. Azim, S. P. Rahman, M. F. Habib and M. A. Hoque, "Estimation of Direction of Arrival (DOA) Using Real- Time Array Signal Processing and Performance Analysis", *IJCSNS International Journal of Computer Science and Network Security*, Vol.10 No.7, pp. 43-57, July 2010.
- 39) A. Abdallah, S.A. Chahine, M. Rammal, G. Neveuxl, P. Vaudont, M. Campovecchio, "A smart antenna simulation for (DOA) estimation using MUSIC and ESPRIT algorithms", 23rd National Radio Science Conference (NRSC 2006), Faculty of Electronic Engineering, Menoufya Univ., Egypt I, March 14-16, 2006.

- 40) K. C. Tan, K. C. Ho and A. Nehorai, "Linear Independence of Steering Vectors of an Electromagnetic Vector Sensor", *IEEE transactions on signal processing*, Vol. 44, No. 12, pp. 3099-3107, December 1996.
- 41) T.B. Lavate, V.K. Kokate, A.M. Sapkal, "Performance Analysis of MUSIC and ESPRIT DOA Estimation algorithms for adaptive array smart antenna in mobile communication", Proceedings second international conference on computer and network technology, ICCNT 2010, Bangkok, Thailand, 23-25 April 2010.
- 42) R. Kawitkar, "Performance of Different Types of Array Structures Based on Multiple Signal Classification (MUSIC) algorithm", Fifth International Conference on MEMS, NANO, and Smart Systems [electronic resource], Proc., Dubai, UAE, pp 159-161, 28-3-December 2009.
- 43) S. Rani, P.V. Subbaiah, K.C. Reddy, "Music and LMS algorithms for a smart antenna system", ET-UK International Conference on Information and Communication Technology in Electrical Sciences (ICTES 2007), Dr. M.G.R University, Chennai, Tamil Nadu, India, pp 965-969, Dec. 20-22, 2007.
- 44) Q. H. Liu and L. H. Zou, "Signal Eigenvectors Decomposition and Direction of Arrival Estimation", International Conference on Circuits and Systems, pp. 344-347, June 1991, Shenzhen, China.
- 45) S.Y. Hou, S.H. Chang, H.S. Hung and J.Y. Chen, "DSP-Based implementation of a real-time DOA estimator for underwater acoustic sources", *Journal of Marine science and technology*, Vol. 17, No. 4, pp. 320-325, 2009.

- 46) M.C Hua, C.H. Hsu and H.C. Liu, "Implementation of direction of arrival estimator on software defined radio platform", *Communication Systems, Networks and Digital Signal Processing (CSNDSP)*, 2012 8th International Symposium, 18-20 July 2012.
- 47) H.Wang and M. Glesner, "Hardware implementation of smart antenna systems", *Adv. Radio Sci.*, 4, 185–188, 2006.
- 48) J. Bermudez, R. C. Chin, P. Davoodian, A. T. Y. Lok, Z. Aliyazicioglu and H. K. Hwang, "Simulation Study on DOA Estimation using ESPRIT Algorithm", *Proc. of the World Congress on Engineering and Computer Science 2009*, Vol. 1, WCECS 2009, San Francisco, USA, October 20-22, 2009.
- 49) C. R.Dongarsane and A.N.Jadhav, "Simulation study on DOA estimation using MUSIC algorithm", *International Journal of Technology And Engineering System (IJTES)*, Vol. 2, No. 1, pp 54-57, Jan – March 2011.
- 50) M. Pesavento, A. B. Gershman and M. Haardt, "Unitary Root-MUSIC with a Real-Valued Eigendecomposition: A Theoretical and Experimental Performance Study", *IEEE transactions on signal processing*, Vol. 48, No. 5, pp 1306-1314, May 2000.
- 51) A. Nehorai and E. Paldi, "Vector-Sensor Array Processing for Electromagnetic Source Localization", *IEEE transactions on signal processing*, Vol. 42, No. 2, pp 376-398, February 1994.